UNIVERSITY OF
CALGARY

The author of this thesis has granted the University of Calgary a non-exclusive license to reproduce and distribute copies of this thesis to users of the University of Calgary Archives.

Copyright remains with the author.

Theses and dissertations available in the University of Calgary Institutional Repository are solely for the purpose of private study and research. They may not be copied or reproduced, except as permitted by copyright laws, without written authority of the copyright owner. Any commercial use or publication is strictly prohibited.

The original Partial Copyright License attesting to these terms and signed by the author of this thesis may be found in the original print version of the thesis, held by the University of Calgary Archives.

The thesis approval page signed by the examining committee may also be found in the original print version of the thesis held in the University of Calgary Archives.

Please contact the University of Calgary Archives for further information,
E-mail: uarc@ucalgary.ca
Telephone: (403) 220-7271
Website: http://www.ucalgary.ca/archives/

UNIVERSITY OF CALGARY

A Study of the Effects of Left Ventricular Contractility and Coronary Tone on Coronary Flow Dynamics using Wave Intensity Analysis

by

Yi-Hui Sun

A THESIS

SUBMITTED TO THE FACULTY OF GRADUATE STUDIES

IN PARTIAL FULFILMENT OF THE REQUIREMENTS FOR THE DEGREE

OF DOCTOR OF PHILOSOPHY

DEPARTMENT OF CARDIOVASCULAR/RESPIRATORY SCIENCES

CALGARY, ALBERTA

JUNE, 2001

© Yi-Hui Sun 2001

ABSTRACT

Coronary blood flow is determined by both upstream aortic events and downstream coronary microcirculatory events. Wave intensity analysis, which separates upstream from downstream events and defines their interaction, has been used to investigate: 1) the mechanisms by which coronary blood flow decreases during systole while coronary pressure increases; and 2) the effects of contractility and coronary tone on the coronary systolic flow impediment. We measured left circumflex coronary, aortic, and left ventricular pressure and left circumflex coronary flow velocity. Wave intensity analysis was applied to identify the determinants of coronary pressure and velocity. During left ventricular isovolumic contraction, coronary pressure is higher than aortic pressure. Increasing left ventricular contractility by paired pacing increases the pressure difference between coronary pressure and aortic pressure. During this time, wave intensity analysis identified a backward-travelling compression wave that increased coronary pressure and decreased coronary flow velocity. This backward-travelling compression wave was augmented by paired pacing. Coronary flow was governed by the interaction between upstream and downstream events. LV ejection caused a forward-travelling compression wave. When it became dominant, it caused coronary flow velocity to increase, despite LV pressure and elastance continuing to increase. Coronary tone was modulated by intracoronary infusion of vasodilators (adenosine, nitroglycerin) and a vasoconstrictor (phenylephrine). At constant contractility, decreasing coronary tone by vasodilators increased the coronary systolic flow impediment and when coronary tone was

increased by the vasoconstrictor, the coronary systolic flow impediment was decreased. Thus changes in the coronary systolic flow impediment were inversely related to the changes of coronary tone. At a constant level of coronary tone, increasing LV contractility increased the coronary systolic flow impediment. When both LV contractility and coronary tone were changed, the largest coronary systolic flow impediment was reached at the highest level of contractility and the lowest level of coronary tone. The energy carried by the backward-travelling compression wave is proportional to the reduction in coronary flow during systole.

ACKNOWLEDGEMENTS

There are many people to whom I wish to express my gratitude and without whom I could not have succeeded in this endeavour.

First and foremost, I would like to thank Dr. John Tyberg, my supervisor and mentor, who provided me with the opportunity to conduct cutting-edge cardiovascular research in his lab. He taught me many things, the most important of which was how to think logically in order to solve problems. Thank you Dr.Tyberg, for leading me to this wonderful world of coronary networks and filled with waves. Your support, kindness, understanding and encouragement throughout my program were fundamental to my success. You made my dream come true. I am unable to define all that you have done for me and I am sure what I have learned in the past few years will continually influence me in my future life.

Dr. Todd Anderson and Dr. William Whitelaw, my Supervisory Committee members, were also very supportive in my research project. They provided valuable suggestions in order for me to resolve problems as they arose and ensured that I was on track throughout all stages of my project. Thank you, Dr. Anderson, for all the time you have spent in the lab with me for my experiments. Without your help I would not able to finish my study.

I would also like to thank other members of our laboratory, Gerry, Cheryl, Rozsa, and John, for providing much-needed assistance in the technical areas such as instrumentation, experimental procedures, data analysis and computer programming.

Thank you, Gerry, for all the help you have given to me from the first day I came to Canada--actually you started to help me even before I came. Thank you, Cheryl, for not only your excellent surgical help but also your understanding and kindness. Thank you, Rozsa, I cannot remember how many times I called you at the weekend. You can always solve my problems. John, without your magical hands my computer never works. Yi-Chun, J.J., Carol, and Jamie were always a pleasure to work with and added significantly to the working environment in the lab. J.J., thank you for everything you taught me. Yi-Chun, my little sister and colleague, thank you for all your help and your troubles, without you my life would not be so colorful!

I would also like to thank my friend, Deanna, for her assistance over the years, helping me to speak and understand English.

I would like to express my great appreciation to the Medical Research Council of Canada for providing me with a Doctoral Research Award and supporting me during this work.

Love also to my sons, George and Geoffrey. You truly are important for my life. Exams are over. Let's go to the park!

Finally, and most importantly, I would like to thank my husband, Bing, and my family (my parents and my mother-in-law) for their unconditional love and encouragement during this challenging time in my life. This project is a testament to the strength of their exceptional support and kindness. Bing, I love you! Thank you for your understanding and support!

This dissertation is dedicated to my family:

my parents and my mother-in-law

my husband, Bing

my lovely sons, George and Geoffrey

Contents

List of Tables

List of Figures

CHAPTER 1

INTRODUCTION

The heart, as a pump, moves oxygenated blood through the vascular system to supply nutrition to the body as well as to itself by each beat. Coronary blood flow makes it possible for the heart to contract. The coronary circulation is a complicated system because it passes through the beating heart.

Although coronary pressure is similar to aortic pressure, coronary flow differs from aortic flow [48,62] and right coronary blood flow in which maximum flow occurs during systole. Factors contributing to decreased left coronary blood flow during systole have been studied for years. It has been widely accepted that cardiac contraction impedes coronary blood flow, so that systolic arterial flow is small compared to diastolic arterial flow [15,26,52,87,90]. However, for decades, investigators have attempted to understand the exact mechanism behind this systolic coronary flow reduction. Today, researchers are still struggling to find an adequate explanation for coronary systolic flow impediment (CSFI). It also remains unclear how coronary blood flow changes in response to this systolic flow impediment with vasomotor tone change.

To understand the effects of left ventricular contractility and coronary tone on coronary flow dynamics, the structural aspects and characteristics of coronary circulation must be understood. After brief descriptions of the anatomy and the regulation of coronary blood flow, the historical development of our understanding of the effects of left ventricular contraction on coronary blood flow will be reviewed.

1.1 Characteristics of the Coronary Circulation

1.1.1 Structure of the Coronary Network

Coronary arteries, arising from the coronary sinuses immediately beyond the aortic valve, supply blood to the highly non-uniform heart with a variable range of demands. There are two major coronary arteries: the left coronary and the right coronary artery. They mainly perfuse the left ventricle, septum and right ventricle respectively (The posterior descending branch of the right coronary supplies the posterior septum). The two main branches of left coronary artery are the left anterior descending artery (LAD) and the left circumflex (LCx). The coronary veins drain blood out of the heart.

The arterial tree of coronary circulation consists of larger arteries, smaller arteries and arterioles. In general, all the arteries with diameters larger than 400μm are referred as larger arteries and those with diameters smaller than 400μm but larger than 100μm are considered as small arteries. Arterioles are very small arteries with only one to three layers of smooth muscle cells and their diameters tend to be smaller than 100μm, as illustrated in Figure 1.1 [93]. However, it is the arteries smaller than 400μm in diameter, which includes small arteries and arterioles that are responsible for the control function.

Coronary arteries start from the epicardium, travel deeply through the cyclically contracting myocardial fibers, and reach the endocardium. Then, blood returns back to the epicardium by the veins. Figure 1.2 shows transmural arteries

from the epicardial into the myocardial wall [93]. From the transmural arteries, small arteries and arterioles branch off to perfuse the capillary bed. The density of the arteries in the endocardium is higher than that in the epicardium [25,26,96].

1.1.2 Structure of Left Ventricular wall

The left ventricle is modeled as a thick-walled cylinder composed of concentric cylinder shells. According to Laplace's law, tangential stresses in the wall generate left ventricular pressure. The ventricular wall consists of three myocardial layers: the endocardium, the myocardium, and the epicardium. Myocardial fiber orientation is different in various parts of the wall. The myocardial muscle sheet is arranged into superficial and deep layers. The superficial fibers start from the base of the ventricles to the apex, where they pass deeply to terminate in the papillary muscles. Fibers of the deep layer run a circular course around the ventricle, with some fibers following an S-shaped pattern when they pass from one ventricle to the other. Regional cardiac mechanics are determined by local fiber stress, velocity of sarcomere shortening, generated mechanical power per unit of tissue volume, or intramyocardial pressure. Intramyocardial pressure, determined by fiber stress, fiber orientation and left ventricular geometry, influences coronary flow during cardiac contraction. The degree of myocardial fiber shortening varies in each layer; shortening is greater near the endocardium and less near the epicardium [37,96,97].

1.1.3 The Coronary Circulation

Many investigators have reported that during cardiac contraction, coronary inflow decreases while coronary outflow increases and stress near the endocardium is higher than it is near the epicardium [14,25,92]. Both subepicardial and subendocardial microvessels flow is reversed in early systole [5,47-49]; Throughout the myocardial wall, there is an intramyocardial pressure gradient which is related to left ventricular pressure [4,64,78,97]. This intramyocardial pressure is higher in the subendocardium and lower in the subepicardium. During systole, large blood vessels change less in diameter than small blood vessels [45]. As well, the flow in the subendocardium is lower than in the subepicardium. The endocardial-to-epicardial flow ratio is equal to 1 in diastole, but is 1.5 during systole. The amplitude of the phasic coronary inflow is related to the inotropy of the ventricle[76].

1.2 Regulation of Coronary Blood Flow

The smooth muscle cells in the vessel wall mediate regulation of coronary blood flow. Regulation of coronary circulation consists of all the mechanisms that play a role in feedback between cardiac function and coronary flow. In the normal heart, there are three dominant mechanisms that regulate coronary blood flow: (1) metabolic regulation, (2) autoregulation, (3) extravascular compression. In addition, neurohumoral, and myogenic controls also contribute to regulate coronary blood flow. In the last decade, it has been clear that the function of coronary endothelium

plays a critical role in coronary flow regulation, particularly in pathological conditions [23,41,58,99].

1.2.1 Metabolic Regulation

A number of substances involved in tissue metabolism affect smooth muscle tone, thus changing coronary blood flow, the most important being oxygen, adenosine, carbon dioxide, pH, and potassium. There is a close link between coronary blood flow and myocardial oxygen consumption [6,19-21,30]. Oxygen consumption is an index of metabolic rate. Coronary blood flow varies to meet myocardial oxygen demand. The partial pressure of oxygen influences the contractile activity of coronary vascular smooth muscle. Decreased partial pressure of oxygen causes vasodilatation. A number of studies have shown that increased oxygen consumption, such as with exercise, increases coronary blood flow [106,115]. Studies have shown that adenosine and K^+_{ATP} channels play an important role in regulating coronary blood flow [82,83,100,114]. Adenosine causes significant increases in coronary blood flow, and, with K^+_{ATP} channel blockade, coronary vasodilatation is inhibited. In recent years, endothelium-derived factors, especially nitric oxide (NO), have proven to be important substances in regulating coronary blood flow[32,32,50,59,59,69,70]. They are involved in flow-mediated dilatation and shear-stress induced vasomotor change [98,99]. NO-mediated coronary vasodilatation may be an important mechanism of metabolic coronary flow regulation.

1.2.2 Autoregulation and Myogenic Controls

The coronary circulation exhibits an autoregulatory response. In the range of 80-150 mmHg, increased perfusion pressure will raise coronary resistance and makes the increase in coronary flow smaller than would otherwise be expected. The range of this regulation is not the same throughout the ventricular wall; it is 40-150 mmHg in the epicardial regions and only 70-150 mmHg in the endocardial regio. Myogenic tone is altered by changing pressure alone. It has been shown that coronary resistance vessels have the intrinsic ability to change coronary blood flow such that autoregulation may be achieved.

1.2.3 Extravascular Compression

Extravascular force increases coronary resistance by compressing coronary vessels. Extravascular compression is directly related to intramyocardial pressure which is determined by ventricular contraction [17,91].

1.2.4 Neural and Humoral Control

Neurohumoral control also contributes to coronary flow regulation. Coronary arteries are well supplied with both sympathetic and parasympathetic nerve fibers. Neural control of coronary vessels mainly affects coronary blood flow, coronary vascular resistance, and large coronary diameter. Reflex effects of natural stimuli act through baroreceptors, chemoreceptors or cardiopulmonary receptors. Sympathetic stimulation causes coronary vasoconstriction, and vagal stimulation causes a mild dilation [22,65]. Both β_1- and β_2-adrenergic receptors are present in the coronary

circulation and can be activated to produce vasodilatation. The ratio of β_1: β_2 adrenergic receptors in large vessels is approximately 1.5-2:1, but in the resistance vessels β_2 receptors are dominant [66,109]. There appears to be a functional distribution of both α_1- and α_2-adrenergic receptors in coronary resistance vessels [13]. When the perfusion pressure was maintained below physiologic levels, autoregulatory responses to pressure change were eliminated and both α_1- and α_2-adrenergic vasoconstriction were unmasked [13]. The endothelium plays an important role in the humoral control of the coronary circulation. Vasoconstrictor responses to α_1- and α_2-adrenergic agonists were attenuated by endothelium-dependent release of nitric oxide [40].

1.3 Historical Development of our Understanding of the Effects of Left Ventricular Contraction on Coronary Blood Flow

The effects of myocardial contraction on coronary blood flow have received much attention in the last century. A number of studies have been conducted in this area. In trying to understand the mechanisms by which coronary flow is reduced during systole, several models have proposed.

1.3.1 Models of Coronary Systolic Flow Impediment

Based on the original observations of Sabiston and Gregg, many experiments have been conducted to understand the effects of cardiac contraction on coronary

flow. Several models have been proposed to explain what happens to coronary blood vessels and to predict coronary blood flow during contraction. The best-known models are the vascular waterfall and the intramyocardial pump. Recently, a time-varying elastance model proposed by the Westerhof group has attracted the attention of researchers.

1.3.1.1 Waterfall model

1.3.1.1.1 Concept

The first model describing the effect of cardiac contraction on coronary blood flow was based on the vascular waterfall mechanism originally introduced by Permutt and Riley and first proposed by Downey and Kirk [27]. Figure 1.3 illustrates the basic principles of this model. The top panel shows a collapsible walled vessel surrounded by a pressure, P_T. The middle panel graphically shows the flow in this system, in which the flow is proportional to perfusion pressure, P_A. If P_T is greater than zero, the flow stops until P_A exceeds P_T. This is because the greater pressure outside the vessel causes it to collapse. When P_T is between P_A and P_V, the vessel collapse occurs at the point where the pressure within the vessel falls below P_T. The high resistance of the partially collapsed vascular segment causes the pressure to decrease from P_T to P_V. Flow becomes a linear function of P_A - P_T with the same slope as it has when P_T is equal to zero. The bottom panel shows an electrical analogy of this system. Current flow is prevented by the battery and the diode until Va (analogous to P_A) exceeds the battery voltage Vt (analogous to P_T).

Downey and Kirk proposed a more complex model as shown in Figure 1.4 [27]. This model represented parallel legs in the coronary vessels at different depths in the

heart wall. "A" is near the endocardium and "D" is near the epicardium. Increased battery voltage indicates increasing intramyocardial pressure across the heart wall with myocardial depth. The bottom of Figure 1.4 illustrates that when V_A exceeds the highest battery voltage (90v), the function is linear below 90 v the line curves toward the left. The broken line shows the results when all of the battery voltages are reduced to zero. Animal experiment results match the theoretical model prediction as shown in Fig. 1.5. The waterfall model demonstrates that tissue pressure varies with depth and shows that the deeper the myocardial layer, the less the current at the same perfusion pressure. The effect of cardiac contraction is to shift the pressure-flow curve to the right. The basic mechanism is the creation of vascular waterfalls where the segments downstream are partially collapsed by local tissue pressure. As we know, coronary arteries start over epicardial surfaces, sending branches perpendicularly into the underlying myocardium. The deeper the arteries go, the higher the pressure surrounding them. Arteries reach their deepest point at the capillaries in the endocardial layer, where the highest intramyocardial pressure occurs[60,97,105]. The main feature of the waterfall mechanism is that cardiac contraction creates an intramyocardial pressure gradient in the ventricular wall. This intramyocardial pressure partially collapses the distal coronary artery and then forms a vascular waterfall which decreases coronary systolic inflow.

1.3.1.1.2 Model evaluation

The waterfall model was proposed to describe the non-autoregulatory coronary bed. In this model, the only variable related to cardiac contraction is intramyocardial pressure which is proportional to left ventricular pressure and

determines the driving pressure, as described by others [79,96]. The model correctly predicts the mean pressure-mean flow graph for the coronary bed (maximally dilated) of the beating and arrested heart. The advantage of the waterfall model is that it explains the decrease in time-averaged flow due to contraction of the ventricle. However, it does not predict the magnitude of the systolic-diastolic change in coronary arterial flow. In addition, the waterfall model cannot explain that systolic coronary flow can be zero or even retrograde when the coronaries are perfused at constant pressure [38,73,85] and that coronary sinus flow is largest in systole [81]. The waterfall model cannot explain these facts because it also assumes that in the epicardial layers the tissue pressure is small. Therefore, the waterfall model always produces significant forward flow, even when flow in the subendocardium has stopped.

1.3.1.2. Intramyocardial Pump Model

1.3.1.2.1. Concept

On the basis of observations that negative systolic flow occurs when perfusion pressures are less than 65 mmHg and the largest venous flow occurs during systole, Spaan [95] proposed the intramyocardial pump model. Fig. 1.6 shows the principle of this concept. It is clear that a change in the tissue pressure is transmitted to the blood contained in the tube. When corks are removed, blood will flow out of both ends because of a blood pressure gradient. This blood flow causes a decreased blood volume in the vessel and is also impeded by viscous forces that form a resistance. Tissue pressure created by cardiac contraction is the driving force for this flow, and

the respective resistances opposing the flow at each end determine the flow amplitudes.

Figure. 1.7 shows the electrical analogy that demonstrates the intramyocardial pump model [95]. Pp represents perfusion pressure and Rs represents stenosis resistance. Coronary resistance Rc = Ra + Rv, in which Ra and Rv are the coronary resistances impeding phasic flow in the arterial and venous sides of the coronary system. Autoregulation may change Ra and Rv. Displacement of blood out of the vessel will result in a decrease in pressure related to vascular compliance. "In this model capacitance has been included as an expression of the fact that volume which can be expelled is limited, and cannot deliver a dc flow".

The intramyocardial pump model considers systolic compression not only as simply impeding flow but also as pumping blood from the myocardium. This displacement of blood volume contributes transiently to the coronary arterial and venous flow. Then, in systole, coronary arterial flow is decreased and coronary venous flow is increased. Spaan points out that the systole flow impediment is not caused by high coronary resistance but by the pressurized intramyocardial blood compartment due to systolic compression (pumped volume or capacity discharge) cyclically charging and discharging. Intramyocardial capacitance plays a fundamental role in determining the timing and direction of blood flow in coronary microvessels. The model also predicts that diastolic coronary flow is determined by the mean flow plus what was pumped in systole.

The intramyocardial pump model was further modified by Arts and Spaan as a non-linear intramyocardial pump model[94]. The difference is that the vascular volume

changes are assumed to be so large that they affect the resistance of the vascular bed. In this model, resistance is determined in a nonlinear way, by vascular volume (law of Poiseuille). In addition, volume is related to transmural pressure though the transmural pressure-volume curve, according to the nonlinear intramyocardial pump model. Cardiac contraction affects coronary arterial and venous flow in two ways. The first transient effect is caused by displacement of volume from the vascular space remains; this is the same as the linear model. The second effect is the increased resistance caused by decreased vascular volume.

1.3.1.2.2. Model evaluation

The intramyocardial pump model corrects three inconsistencies of the waterfall model: (1) perfusion flow can reverse for small perfusion pressure, (2) when perfusion flow is stopped perfusion pressure still oscillates, and (3) coronary sinus flow is largest in systole. However, because coronary blood flow variations during cardiac contraction result from a capacitive flow, only linear models cannot predict the flow reduction during static contractions as proposed by Bouma [8]. In a nonlinear model, in which cardiac contraction also affects the vascular diameters and then resistance, flow reduction in dynamic contractions is both capacitive and resistive. Since reduction of flow during sustained contractions is only resistive, this model predicts a smaller reduction during sustained contraction than during dynamic contraction.

1.3.1.3. Time-Varying Elastance Model

Both the waterfall and intramyocardial pump models have explained the coronary systolic flow impediment based on the direct and unique coupling of left

ventricular pressure and intramyocardial pressure. Therefore, intramyocardial pressure is related to the coronary flow impediment. Whether left ventricular pressure is changed by volume loading (Frank-Starling mechanism) or by changes in contractility appears to be irrelevant. It has been reported that changes in contractility in the maximally vasodilated coronary bed affect arterial inflow and flow velocity in small subepicardial arteries and veins reversed in early systole [5,63]. These vessels perfuse the subepicardium only and since the effect of cardiac contraction on the subepicardium is small, the effect of intramyocardial pressure should be negligible. Phasic septal arterial inflow was shown to decrease before left ventricular pressure increased [11]. During systolic perfusion, endocardial vessels are more dilated than epicardial vessels [9]. According to other models without left ventricular pressure development in systole, the endocardial-to-epicardial flow ratio should be close to the one observed in diastole, which is about 1 [24,113]. However, the endo-to-epi flow ratio is reported equal to 1.5 [26]. None of these results can be explained by intramyocardial pressure change. This suggests that factors other than extravascular pressure should be taken into account when explaining systolic coronary flow impediment. Westerhof et al. observed that there is a poor relation between left ventricular and intramyocardial pressure [55]; therefore, they hypothesized that properties of the muscle surrounding the coronary vasculature should be taken into consideration.

1.3.1.3.1 Concept

The concept of time-varying elastance has been proposed by Suga et al. [102] as a time-varying ventricular pressure-volume relation. It states that the elastance changes from a low diastolic value to a high systolic value along a fixed course

independently of preload and afterload. However, elastance depends on the contractility of the muscle. Time-varying elastance, E(t), defined as the ratio of pressure to volume, results from the time-varying stiffness of the cardiac muscle. The E(t) concept is described by $E(t)=P(t)/[V(t)-V_d]$ where P is pressure and V is volume. Westerhof et al. proposed that the time-varying elastance concept not only predicts the ventricular pressure-volume relation but also predicts the pressure-volume relation in the coronary circulation [53-56]. The left ventricle is thought to be composed of two compartments, the ventricular lumen compartment and the (lumped) vascular compartment. Both compartments are surrounded by myocardial fibers. The time-varying elastance is an index of the actively changing elastic properties of the muscle fiber and affects both the ventricular lumen and the vascular compartment. Figure 1.8 and Figure 1.9 demonstrate the time-varying elastance concept as it applies to both the left ventricle lumen and the vascular compartment. As shown in Figure. 8A & 8C, for an isovolumic beat and an isobaric beat (low-afterload), end-systolic pressure-volume ratio (E_{max}) is the same. It indicates that in the isovolumic beat the wall deformation (strain) is minimal while wall stress is maximal. On the other hand, in the isobaric beat, wall deformation (strain) is maximal but wall stress is minimal. However, the stiffness varies in an identical way during the cardiac cycle because it depends on both stress and strain.

In the intramyocardial lumped vascular compartment, cardiac contraction increases the stiffness of the myocardial fibers surrounding the intramyocardial vessels. Then, the elastance of the vascular compartment increases because it is determined by the vessel wall and the surrounding myocardium. Increasing elastance

causes increasing pressure and decreasing volume, E = P/V. Furthermore, it increases resistance because vascular resistance is inversely related to the vascular volume squared (law of Poiseuille). The magnitude of the coronary elastance in systole (CE_{max}) is determined by the volume of the vascular compartment. Thus, for the total coronary bed, vascular elastance and resistance are increased by cardiac contraction. When the coronary perfusion and venous pressure are kept constant, the resistance and compliance changes result in a variance in coronary systolic flow. As shown in Figure 1.8, during isovolumic and isobaric cardiac contractions the pressure-volume trajectories are the same. According to this concept, the systolic flow is the same in isovolumic and isobaric beats. Changing cardiac contractility will change the elastance and thus the systolic flow impediment. As shown in Figure 1.9, an increase in contractility increases the E_{max} (from E_{max} 1 to E_{max} 2) and then systolic volume is decreased. The larger E_{max} reflects a small systolic vascular compliance, and the smaller volume reflects a higher systolic resistance. Therefore, increasing contractility causes a more impeded systolic coronary flow.

1.3.1.3.2. Model evaluation

The time-varying elastance model considers the coronary systolic flow impediment to be determined by the elastance of the surrounding myocardium, not left ventricular pressure [56]. The model, strictly speaking, is an intramyocardial pump model; however, the driving force for the pump action is time-varying elastance instead of varying intramyocardial pressure, and intramyocardial blood space is considered as a chamber of the heart. With the time-varying elastance concept,

changes in blood pressure and blood displacement are explained by the analogy of the well-known pressure volume relations of the left ventricle. As in the nonlinear intramyocardial pump model, increased resistance, caused by decreased vascular volume, matches the blood displacement.

According to the time-varying elastance concept, contractility affects the elastance; therefore, it affects coronary systolic impediment. Westerhof et al. conducted a series of experiments and proved the elastance concept [53-56]. Results showed that with increased or decreased contractility, the slope of the end-systolic pressure-volume relation increases or decreases, the CE_{max} line increases or decreases, and thus the coronary blood flow impediment increases or decreases (systolic flow impediment decreases or increases). With a constant contractile state, changing systolic left ventricular pressure does not cause changes in normalized flow amplitude.

The time-varying elastance concept explains phenomena which cannot be explained by the waterfall and intramyocardial pump models such as: (1) pacing the left ventricle at different sites changes coronary inflow [11] because the moment the time-varying elastance starts to change varies with different pacing locations [10]; and (2) subepicardial microvessel flow is reversed in the early systole [5] because increased elastance surrounding the vessels causes increasing coronary resistance and displaced blood. The time-varying elastance model is adequate to explain the impeding effect of cardiac contraction on coronary flow. However, the model still comes up short in some aspects. It is not clear why the pulsation of the right coronary artery flow is

much less than the left coronary artery, while at the microscopic level the interaction between the myocytes and microvessels is much the same.

1.3.2 Model Evaluation

In summary, the waterfall model and intramyocardial pump model predict a strong effect of left ventricular pressure on coronary systolic flow impediment and no effect of perfusion pressure as shown by many investigators. On the other hand, the time-varying elastance model predicts that perfusion pressure and contractility determine the coronary systolic flow impediment, with no effect from left ventricular pressure. It seems that there is no "perfect" model. The waterfall model was designed to interpret the cardiac-impeding effect on time- and space-averaged coronary flow through the myocardial wall, but fell short for the explanation of the magnitude of phasic flow. The intramyocardial pump model was designed to explain the phasic coronary arterial flow signal but proved inadequate in interpreting the time-averaged flow. The time-varying elastance model provides a relationship between myocardial contractility and coronary flow, but it still cannot explain all the phenomena. It is important to know the limitations and predictive power of the different models, and carefully analyze whether the results can be explained by the model under study.

1.4 Description of Chapters in Dissertation

In the following chapter (Chapter 2), a detailed description of wave intensity analysis will be presented. Wave intensity analysis, a new method of analysis, is used to understand coronary flow dynamics in present study. In Chapter 2, the concept of the wave and wave intensity analysis will be described. In addition, the limitations of wave intensity analysis and the advantages of using wave intensity analysis in studying coronary flow dynamic will be discussed.

Chapter 3 will provide the experimental methods utilized in this dissertation in terms of animal preparation, data collection, Doppler delay measurement, data analysis, and statistics.

Chapter 4 describes the adaptation of wave intensity analysis in coronary circulation. In addition, the mechanism of coronary systolic flow impediment is discussed using wave intensity analysis.

Chapter 5 focuses on discussion of the effects of coronary tone and contractility on coronary flow dynamics. First, the results of the effects of changing coronary tone with constant contractility on coronary dynamics will be provided. Then, the effects of changing coronary tone and contractility on coronary flow dynamics will be discussed in terms of wave intensity analysis.

Chapter 6 summarizes the findings of previous chapters. The final chapter discusses suggestions for future research directions using wave intensity analysis to understand coronary flow dynamics in both experimental and clinical investigations.

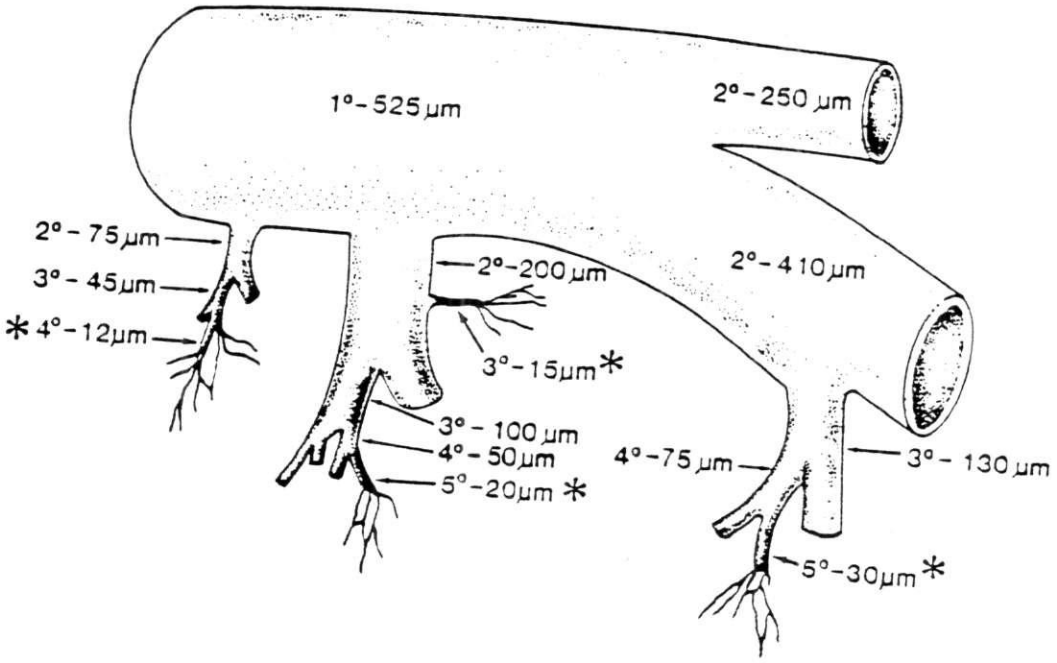

Figure 1.1 Illustration of coronary artery branching patterns.

Figure 1.1 Illustration of coronary artery branching patterns. 1^0 indicate a primary branch; 2^0 indicate the secondary branch, and so forth. "*" indicate terminal arterioles which are 30μm or less in diameter. Reproduced from "Coronary blood flow" by Spaan[100].

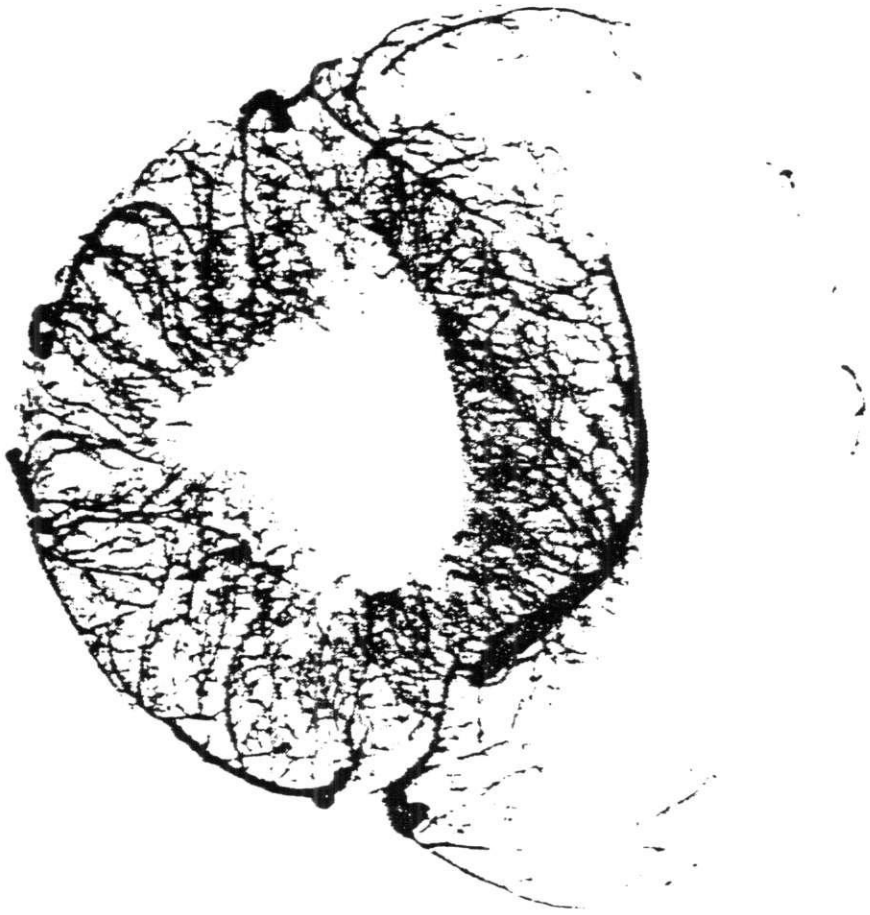

Figure 1.2 Angiogram of a slice of dog myocardium illustrates coronary transmural arteries.

Figure 1.2 Angiogram of a slice of dog myocardium with the arterial tree filled with barium-gelatin mixture. Illustrates coronary transmural arteries that started from the epicardium and reached the endocardium as arterioles. Reproduced from "Coronary blood flow" by Spaan[100].

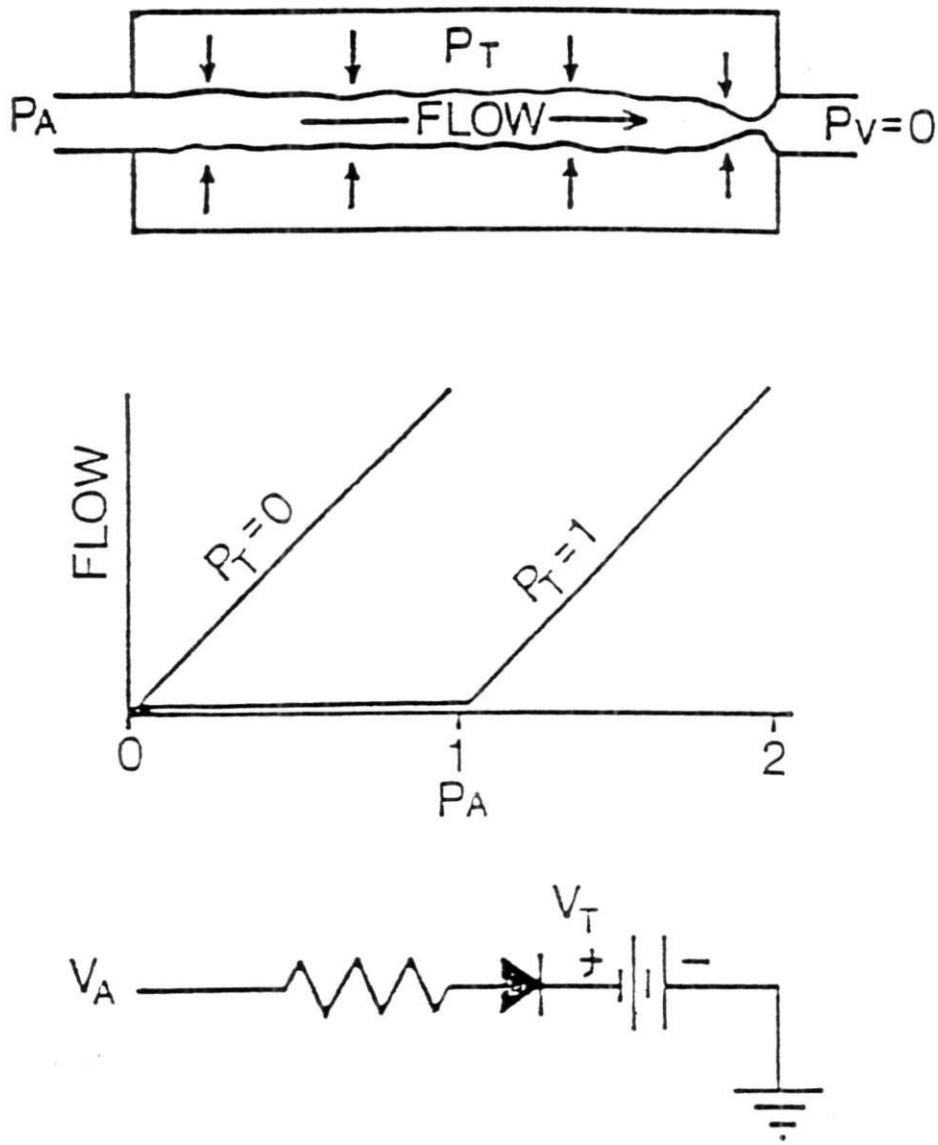

Figure 1.3 Illustration the concept of Waterfall model.

Figure 1.3 Illustration the concept of waterfall model.

Top: A collapsible tube surrounded by pressure P_T. When P_T is greater than outflow pressure P_V but smaller than inflow pressure P_A, a partial regional collapse occurs at the outflow end. **Middle**: Graph of flow as a function of P_A in this system. The line at the left results from P_T=0,and the line at the right results from P_T=1. Bottom: Electrical analogue of waterfall model. The voltage V_A is analogous to P_A, and V_T is analogous to P_T. Current in the circuit is analogous to fluid flow in the model [27].

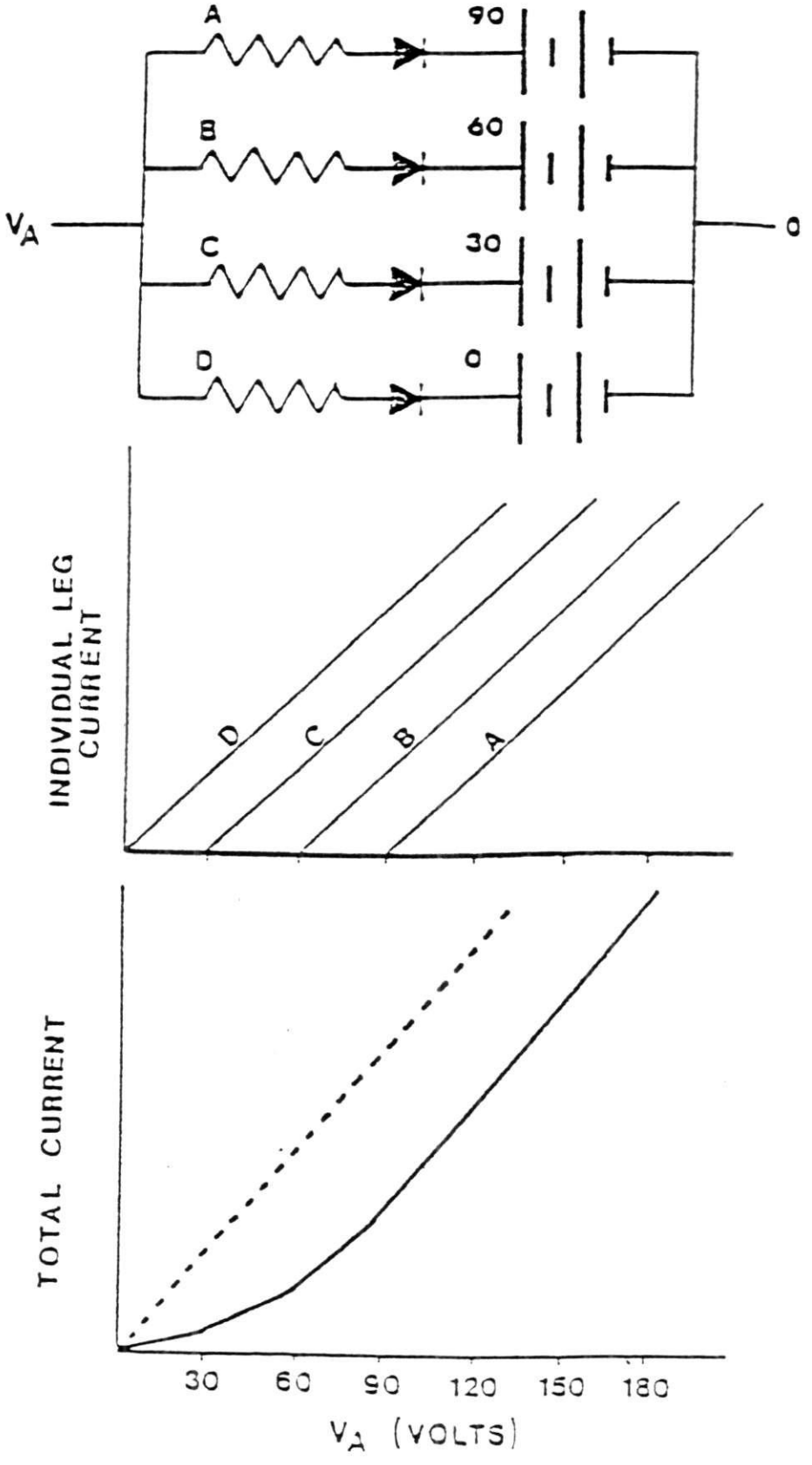

Figure 1.4 A model shows tissue pressure changes with depth.

Figure 1.4 A model shows tissue pressure changes with depth.

Top: Parallel circuit elements, each with a different battery voltage, representing coronary vessels at different depths in the ventricular wall. **Middle**: Individual leg currents as a function of V_A. **Bottom**: The solid line is the total current for the network as a function of V_A, and the broken line shows the current that would occur if the battery voltage were set to zero (represent the state of minimal tissue pressure) [27].

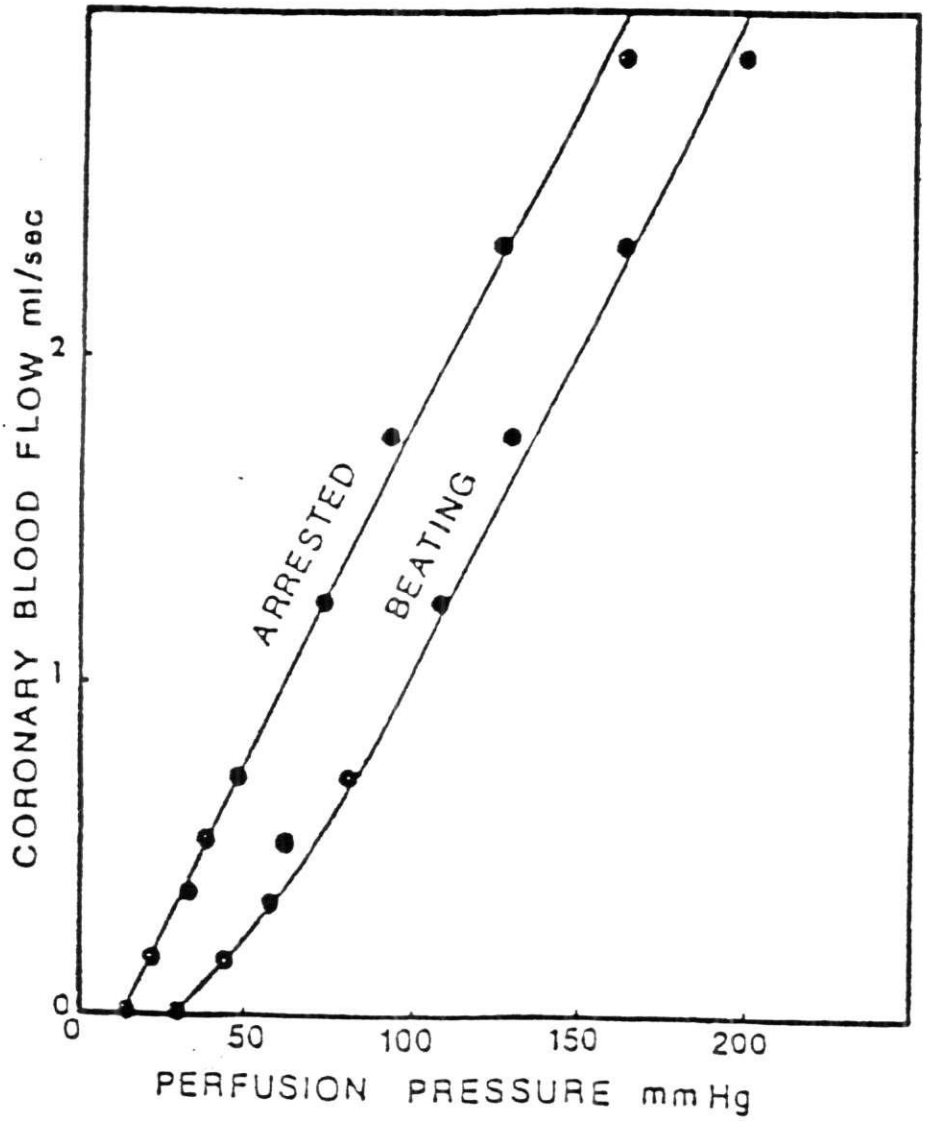

Figure 1.5 Coronary pressure-flow relation in beating and arrested state.

Figure 1.5 Coronary pressure-flow relation in beating and arrested state.

Coronary blood flow plotted against perfusion pressure for the beating state and the arrested state[27].

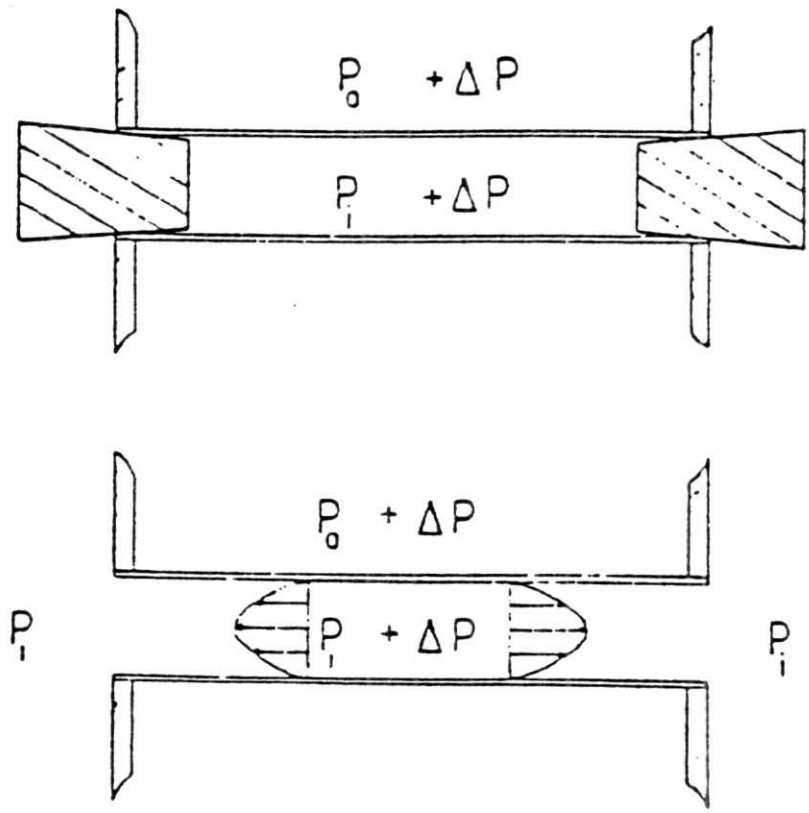

Figure 1.6 Illustration of the principle of the intramyocardial pump.

Figure 1.6 Principle of the intramyocardial pump. **Top:** The pressure within a closed elastic tube, P_i is in equilibrium with the pressure outside, P_o Enlarging P_o by ΔP leads to and increase in Pi also by ΔP. **Bottom**: When the flexible tube is open, ΔP also will be transmitted now causing a flow which is impeded by viscous forces[95].

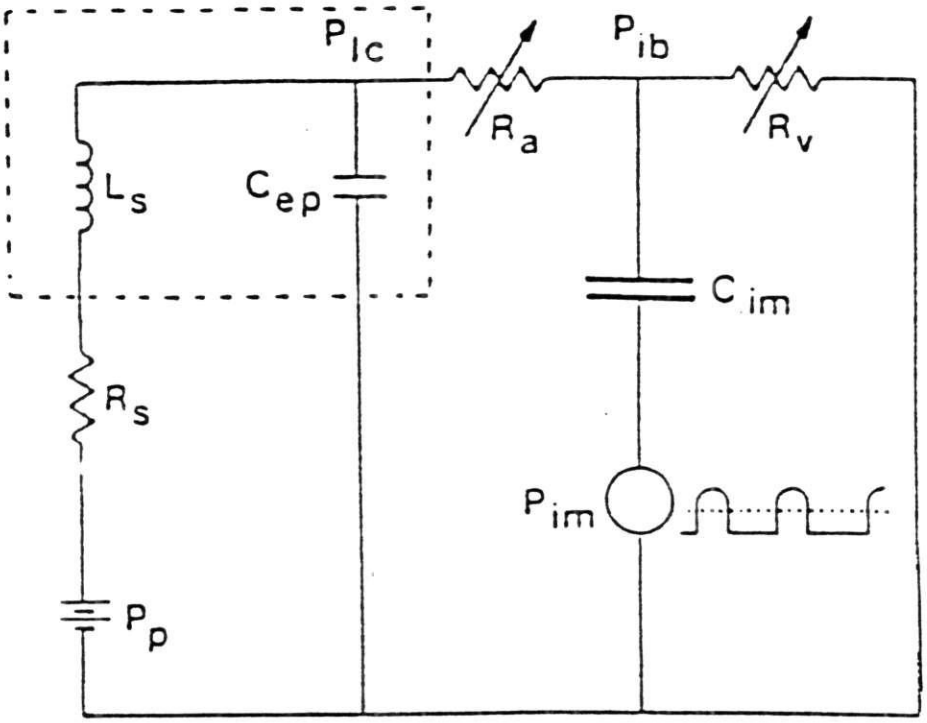

Figure 1.7 Electrical analog showing the intramyocardial pump function.

Figure 1.7 Electrical analog depicting the intramyocardial pump function. P_{im} = intramyocardial tissue pressure, which can be described by the superposition of a d.c. component, P_{im} and an a.c. component, p_{im}. C_{im} = intramyocardial capacitance: R_a and R_v are the coronary resistances impeding phasic flow in the arterial and veous sides of the cornonary system, respectively. Both R_a and R_v may vary due to autoregulation. P_{ib} = intramyocardial blood pressure, which can be described by the superposition of a d.c. component, P_{ib} and an a.c. component, P_{ib}. Since C_{im} is large, $p_{ib} = p_{im}$. P_p = perfusion pressure and R_s = left main coronary artery pressure. The combination of L_s and C_{ep} causes contamination of P_{lc} and coronary blood flow signal

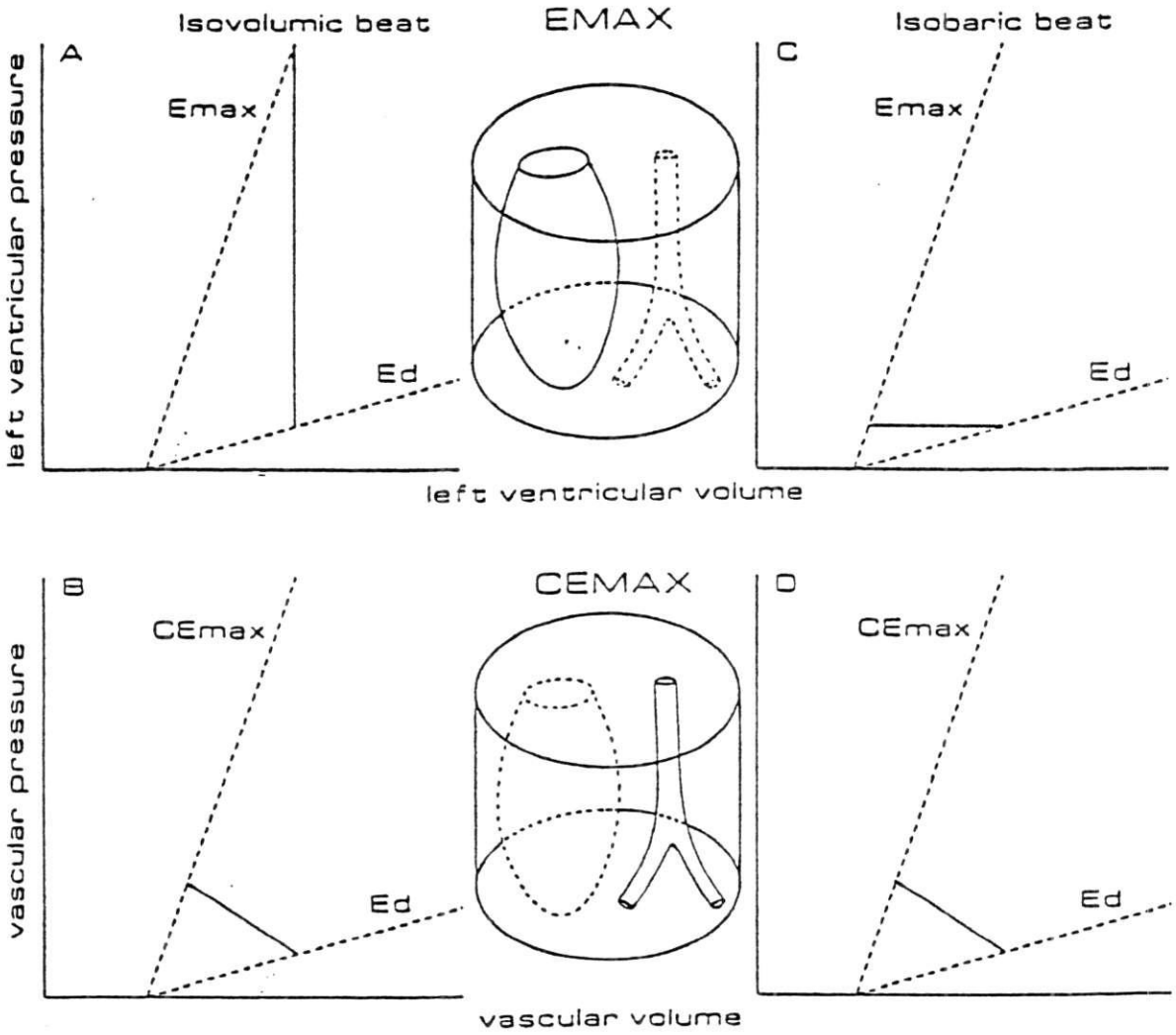

Figure 1.8 Qualitative representation of the left ventriculat lumen compartment and (lumped) vascular compartment (inset).

Figure 1.8 Qualitative representation of the left ventricular lumen compartment and (lumped) vascular compartment (inset). Both lumen and vasculature are contained in the myocardium (represented as a cylinder). Lumen is drawn as ellipsoidal, the vasculature as a branching vessel. Top inset shows concept as applied to left ventricular lumen. Bottom inset shows concept as applied to vascular compartment. Diastolic (E_d) and end-systolic (E_{max}) elastance are drawn as straight lines and pertain to the ventricular lumen. E_d and CE_{max} refer to elastance of coronary system. A: pressure-volume trajectory of left ventricle during isovolumic conditions. B: hypothetical pressure-volume trajectory of coronary intramyocardial vasculature during (ventricular) insovolumic conditions. C: same as A during isobaric conditions. D: same as B during isobaric conditions. B and D are same (see text), i.e., for isovolumic and isobaric beats (left and right, respectively) vasculature is subjected to the same changes[53].

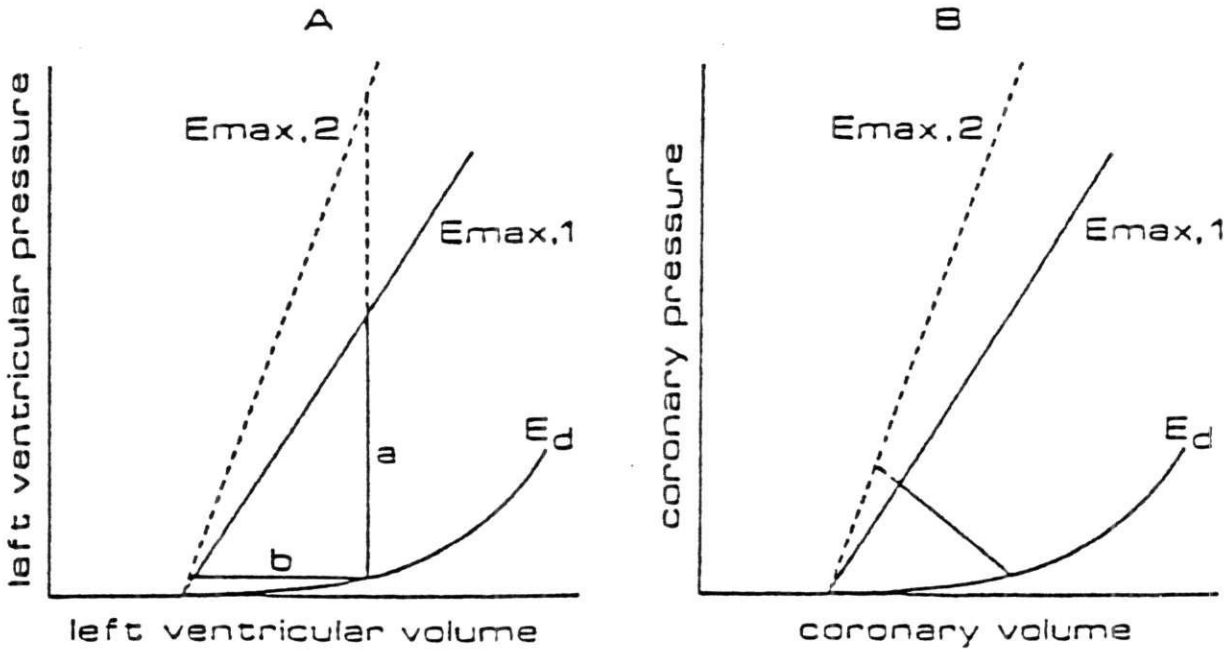

Figure 1.9 Ventricular pressure-volume relation in diastole and systole.

Figure 1.9 Ventricular pressure-volume relation in diastole (E_d) and systole ($E_{max.1}$). For an isovolumic beat (no volume change) the pressure-volume trajectory followed is given by a. For an isobaric beat (no pressure development, large volume change) trajectory b is followed. For both contractions the systolic pressure-volume relations of the vascular compartment is diastole (E_d) and systole ($E_{max.1}$). For a (lumen) isovolumic and (lumen) isobaric beat the trajectory of the vascular compartment is the same since elastance behaves the same and coronary perfusion pressure and venous pressure are the same. An increase in contractility increases the E_{max} (from $E_{max.1}$ to $E_{max.2}$) and therefore systolic volume is decreased. The larger E_{max} corresponds to a smaller systolic vascular compliance, the smaller volume corresponds to a higher systolic resistance. Thus with increased contractility coronary inflow is more impeded.

CHAPTER 2

WAVE INTENSITY ANALYSIS

2.1 The Concept of Wave

A wave is a propagated disturbance [61]. For example, as the left ventricle contracts, it ejects and accelerates its stroke volume into the arterial system, generating a propagated wave, which changes arterial pressure and blood flow velocity.

2.1.1 Types of Wave

Waves can be either forward or backward travelling. A wave that runs from the heart (proximal) towards the periphery (distal) is called a "forward-travelling wave", while a wave that runs from the periphery (distal) towards the heart (proximal) is called a "backward-travelling wave". In general, forward-travelling waves are generated by the heart's contraction and backward-travelling waves are generated by wave reflection.

Waves can be either compression or expansion waves. Regardless of the direction of travel, a wave that increases pressure is called a "compression wave" (there is a greater pressure behind the wave than in front of it, $dP\pm > 0$). A wave that decreases pressure is called an "expansion wave" (there is a greater pressure in front of the wave than the pressure behind the wave, $dP\pm < 0$). Compression waves act as if blowing or pushing; expansion waves act as if sucking or pulling.

There are 4 possible combinations: forward compression, forward expansion, backward compression and backward expansion waves. The effects of a wave on pressure are simple: compression waves always increase pressure and expansion waves always decrease pressure. The effects of compression and expansion

waves on velocity are more complicated: forward-travelling compression waves cause velocity to increase (acceleration, dU+ >0) in the forward direction, while forward-travelling expansion waves cause deceleration (dU+ <0). Oppositely, backward-travelling compression waves cause deceleration (in the forward direction, dU- <0) and expansion waves cause acceleration (dU- >0)[44,74]. The effects of four types of waves on the pressure and flow velocity are summarized in Table 2.1 and an illustration of four types of waves is showed in Figure 2.1.

2.1.2 Physiologic and Familiar Examples

Physiologic and familiar examples of waves are summarized in Table 2.2. A physiologic example of a forward-travelling compression wave is that generated by the contracting heart which accelerates aortic blood at the beginning of ejection [75]. For better understanding, we can think of forward-travelling compression wave as those that are produced by blowing through a straw. A physiologic example of a forward-travelling expansion wave is that generated by the relaxing heart which decelerates aortic blood at the end of ejection. We can think of forward-travelling expansion waves as those that are produced by sucking though a straw. The most familiar physiologic example of backward-travelling compression wave is the aortic reflection wave that generates an anacrotic wave in an older individual. It may be helpful to consider backward-travelling compression waves as those that are produced by a green-to-yellow traffic light change. A physiologic examples of backward-travelling expansion waves are those which are generated by the relaxing left ventricle

and have been identified with left ventricular diastolic suction [107]. The familiar phenomenon is that which is produced by a red-to-green light change.

2.1.3 Wave Speed

The wave speed is how fast the wave travels in a medium. It is the speed by which the change in velocity or pressure propagates along a given segment of vessel. Sir Isaac Newton determined the wave speed to be dependent upon the elasticity and the density of that medium. Further on, Young defined the pulse wave speed as the change in pressure and distensibility of a given arterial vessel [68]. Later Kortweg proposed the well-known equation for wave speed in an elastic tube:

$$C = \sqrt{\frac{Eh}{D\rho}} \qquad (2.1)$$

where E is Young's modulus, h is wall thickness, D is the internal diameter and ρ is blood density. Three assumptions are applied to this equation:

1. h is very small with respect to D
2. The tube is distensible
3. The fluid is incompressible

The systemic arterial system meets these three assumptions reasonably well. Thus, wave speed in arterial vessels is mainly determined by the properties of the local arterial wall.

2.2. The Concept of Wave Intensity Analysis

2.2.1 Theoretical Base

The theory of wave intensity analysis is based on the idea that each wave causes a change in pressure, dP, and a change in velocity, dU. Wave intensity analysis is based on the method of characteristics, through which the energy transported by a wave can be quantitated by measuring the differences in pressure and velocity across the wavefront[61]. Because the wave is propagating in space and time, this pressure and velocity difference produce both spatial gradients and temporal changes at a fixed location.

2.2.2 Separation of Waves

At any location, the measured pressure or velocity depends upon the contributions of any forward or the backward-travelling waves. If we assume that the waves intersect in a linear fashion, the change of pressure and velocity at the point of intersection is the algebraic sum of the change of pressure and velocity due to the forward wave, and the change of pressure and velocity due to the backward wave. In other words, in a one-dimensional wave system, the instantaneous values of pressure and velocity at any time and location are determined by the interaction of forward and backward-travelling waves. Thus,

$$dP = dP_+ + dP- \qquad (2.2)$$

$$dU = dU_+ + dU- \qquad (2.3)$$

Where "+" refers to the forward and "-" refers to backward running waves.

An example of the integration of aortic dP+ and dP- is shown in Figure 2.2. Thus, each measured wave is the result of forward- and backward-travelling waves and actually represents wave interaction.

When the wave speed is known, the effect of a pressure pulse on the blood's velocity is described as:

$$dP_{\pm} = \pm \rho \, c \, dU_{\pm} \qquad (2.4)$$

When the wave speed is known, the pressure and velocity differences across the forward and backward waves can be calculated as:

$$dP_{+} = \tfrac{1}{2} (dP + \rho \, c \, dU) \qquad (2.5)$$

$$dP_{-} = \tfrac{1}{2} (dP - \rho \, c \, dU) \qquad (2.6)$$

$$dU_{+} = \tfrac{1}{2} (dU + dP/\rho \, c) \qquad (2.7)$$

$$dU_{-} = \tfrac{1}{2} (dU - dP/\rho \, c) \qquad (2.8)$$

where ρ is the density of blood, c is the wave speed, dP is the incremental difference in measured pressure and dU is the incremental difference in measured velocity.

2.2.3 Wave Intensity Analysis

WIA was first used by Parker and Jones to study ventriculo-arterial interactions in 1990 [74]. WIA was developed by solving non-linear one-dimensional equations of motion and is based on the concept that "waves" (i.e., propagated disturbances) travel through the vasculature and are manifested by changes in pressure and velocity [44]. Wave intensity is the rate of energy (per unit area) transported by the wave. It is calculated as:

$$dI_W = (dP_+^2 - dP_-^2)/\rho c \qquad (2.9)$$

The mks unit of wave intensity is W/m^2

In terms of measured pressure and velocity, (net) wave intensity also can be calculated by multiplying the incremental change in measured pressure times the incremental change in measured velocity.

$$dI_W = dP*dU \qquad (2.10)$$

Intensity of forward-travelling and backward-travelling waves is calculated from measured pressure and velocity changes:

$$dI_{W+} = \tfrac{1}{4}(dP + \rho c dU)^2 \qquad (2.11)$$

$$dI_{W-} = \tfrac{1}{4}(dP - \rho c dU)^2 \qquad (2.12)$$

Thus, from equations **2.10, 2.11** and **2.12** we will see that the relationship between wave intensity (dI_W, net wave intensity) with forward-travelling wave intensity (dI_{W+}) and backward-travelling wave intensity (dI_{W-}) is described as:

$$\mathbf{dI_W = dI_{W+} + dI_{W-}} \qquad \mathbf{(2.13)}$$

Wave intensity has two components: the intensities of the forward-travelling (dI_{W+}) and the backward-travelling waves (dI_{W-}). dI_{W+} and dI_{W-} directly represent the respective upstream and the downstream effects at any location, while the net intensity (dI_W) reflects the net effects of the forward- and backward-travelling waves. In fact, when backward- and forward-travelling waves interact each other, the measured wave intensity (dI_W) is the algebraic sum of the intensities of two waves interacting. When dIW is positive ($dI_W > 0$), the forward-travelling wave is dominant; when dI_W is negative ($dI_W < 0$), the backward-travelling wave is dominant. If dI_W is very small, it may either mean that there is little wave movement or that the value of the intensities of the forward- and backward-travelling waves are similar at that time and position.

To determine whether a wave is compression or expansion, the pressure differences across the forward-travelling waves (dP_+) and across the backward-travelling waves (dP-) are calculated using equation **2.5** and **2.6**. When $dP_+ > 0$, the forward-travelling wave is a compression wave. Oppositely, $dP_+ < 0$ indicates a forward-travelling wave expansion wave. When dP. > 0, the backward-travelling wave is a compression wave. Oppositely, dP- < 0 indicates a forward-travelling wave

expansion wave. Figure 2.3 demonstrates how net wave intensity (dPdU) is calculated from aortic pressure and flow.

The energy of the wave, I_{W+} (forward) or I_{W-} (backward), can be obtained by integrating the area under the respective intensity waveform.

$$\mathbf{I_{W+} = \int (dI_{W+})\, dt} \qquad \mathbf{(2.14)}$$

$$\mathbf{I_{W-} = \int (dI_{W-})\, dt} \qquad \mathbf{(2.15)}$$

The unit of I_W is J/m^2

WIA can calculate wave speed (c) from measured pressure and velocity:

$$\mathbf{C = 1/\rho(\, dP/dU)} \qquad \mathbf{(2.16)}$$

This equation is only valid for unidirectional waves. Therefore, it should be used when there is little likelihood that opposite waves exists (e.g., very early in systolic ejection).

2.3 The Advantage of Using Wave Intensity Analysis in Studying Coronary Flow Dynamics

WIA provides information regarding the direction, intensity, and type of travelling waves present at any given moment and location in a blood vessel [42,74,75].

Because WIA is a time-domain analysis, wave intensity can be related temporally to hemodynamic parameters and beat-to-beat analyses can be performed [44,74]. Net wave intensity can be calculated relatively easily from real time data, requiring no assumption of periodicity or knowledge of the wave speed. Furthermore, the transient events can be studied. WIA has the convenient property that it is positive for all forward-travelling waves and negative for all backward-travelling waves.

Coronary pressure and flow velocity are determined by both upstream aortic effects, which are related to left ventricular function and the properties of systemic circulation, and by downstream microcirculatory effects, which are related to left ventricular function and coronary vascular properties. WIA discriminates upstream events from downstream and represents their interaction. In addition, WIA is a very sensitive tool that provides further information whether the forward- or backward-travelling wave is a compression or expansion wave. For example, it might have been shown that the reflected waves were expansive rather than compressive when the caliber of proximal conducting arteries was increased. Thus, we believed that WIA would be a suitable and helpful tool for studying coronary flow dynamics.

2.4 Limitations of Wave Intensity Analysis

Wave intensity analysis is a useful method to studying flow dynamics. However, there are some limitations.

1. Wave speed depends on the properties of arteries wall. It varies in different conditions and at different locations. When separated wave intensity is calculated, using the appropriate wave speed value is very important. Although

net intensity can be determined without wave speed, so much more information is available after wave separation. It is practical difficult to calculate wave speed when there is only a small interval without backward waves; also, the delay in velocity measurements compounds the difficulty.

2. Wave intensity analysis requires that the pressure and the velocity be measured at the same location. Unless satisfactory approximations can be made, this may limit the use of wave intensity analysis in clinical studies.
3. Magnitude of wave intensity depends on the values of the first derivative of the pressure and the velocity at a specific time and location. Therefore, variable magnitudes of wave intensity are obtained using different sampling frequencies, although the shape of the curve will not be changed. Thus, it is important that when carrying out a comparison between different studies using WIA, the sampling frequency should be known and the data will need to be normalized.

Table 2.1 Effects of wave on pressure and velocity

Forward Wave (+ dIW)

Compression (blowing): ↑ P, ↑ U

Expression (sucking): ↓ P, ↓ U

Backward wave (- dIW)

Compression (blowing): ↑ P, ↓ U

Expression (sucking): ↓ P, ↑ U

Table 2.2 Summary of physiologic and familiar examples of forward- and backward–travelling waves

Wave Type	Physiologic	Familiar
Forward compression wave	Acceleration of aortic blood (increasing LV elastance)	Blowing through a straw
Forward expansion wave	Deceleration of aortic blood (decreasing LV elastance)	Sucking through a straw
Backward compression wave	(aortic) anacrotic wave (reflection from periphery)	Green- to-yellow light change
Backward expansion wave	LV diastolic suction (decreasing LV elastance)	Red – to –green light change

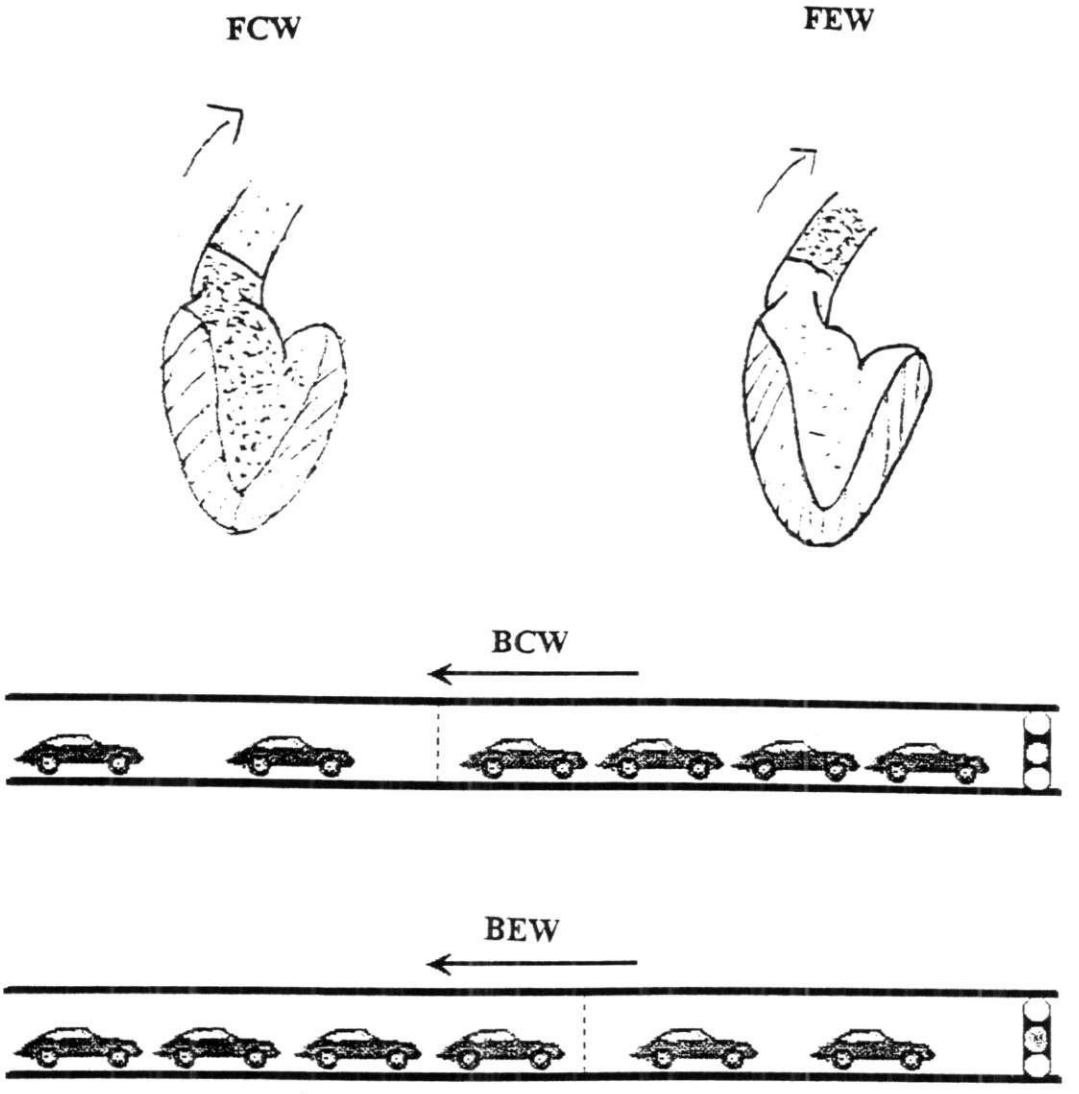

Figure 2.1 Illustration of examples of forward- and backward-travelling compression and expansion waves

Figure 2.1 Illustration of examples of forward- and backward-travelling compression and expansion waves. A forward-travelling compression wave is produced by the contracting LV; while a backward-travelling expansion wave is produced by the relaxing LV. A backward-travelling compression is produced by a green –to- yellow traffic light change while a backward-travelling expansion wave is produced by a red-to-green traffic light change.

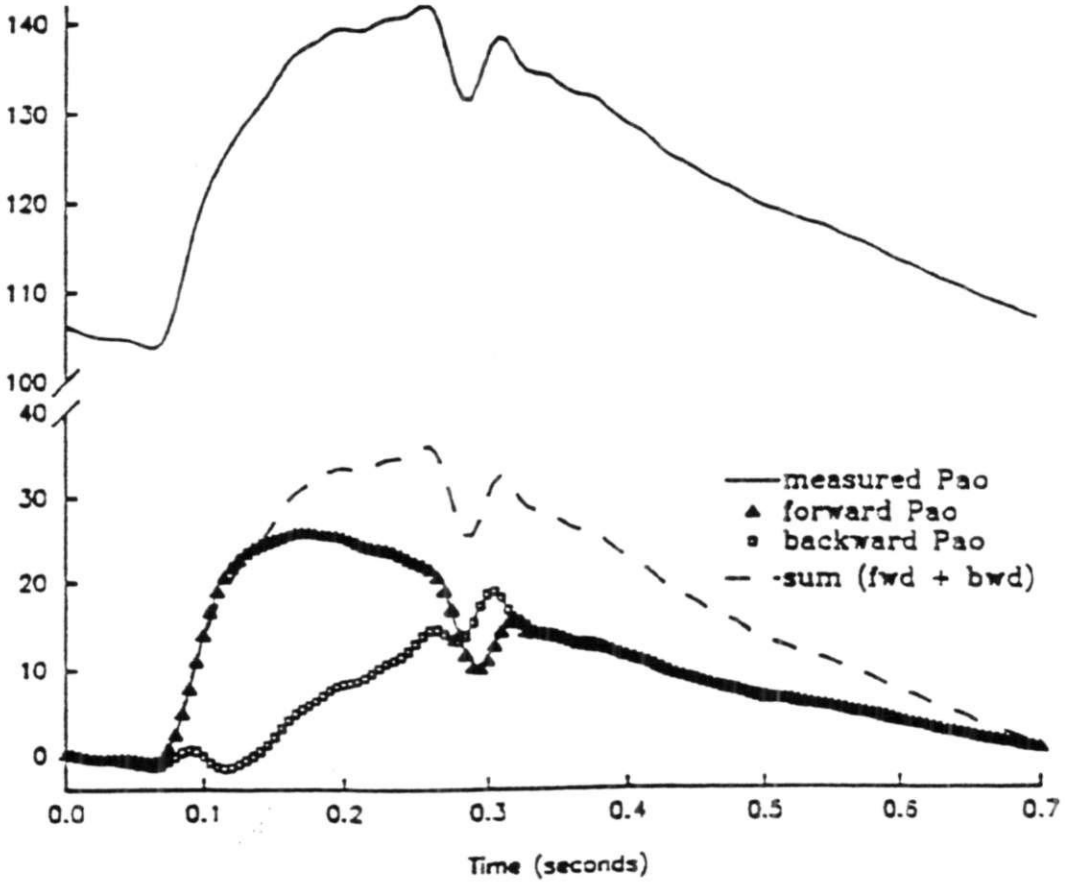

Figure 2.2: Components of a Typical Measured Aortic Pressure Wave

Figure 2.2 Components of a typical measured aortic pressure waveform.

Each measured aortic pressure waveform is considered as the summation the waveforms derived by integrating dP+ and dP- of the respective forward- and backward-travelling waves. The forward component is due to LV systolic ejection and the backward component is due to reflected waves which return toward the ventricle.

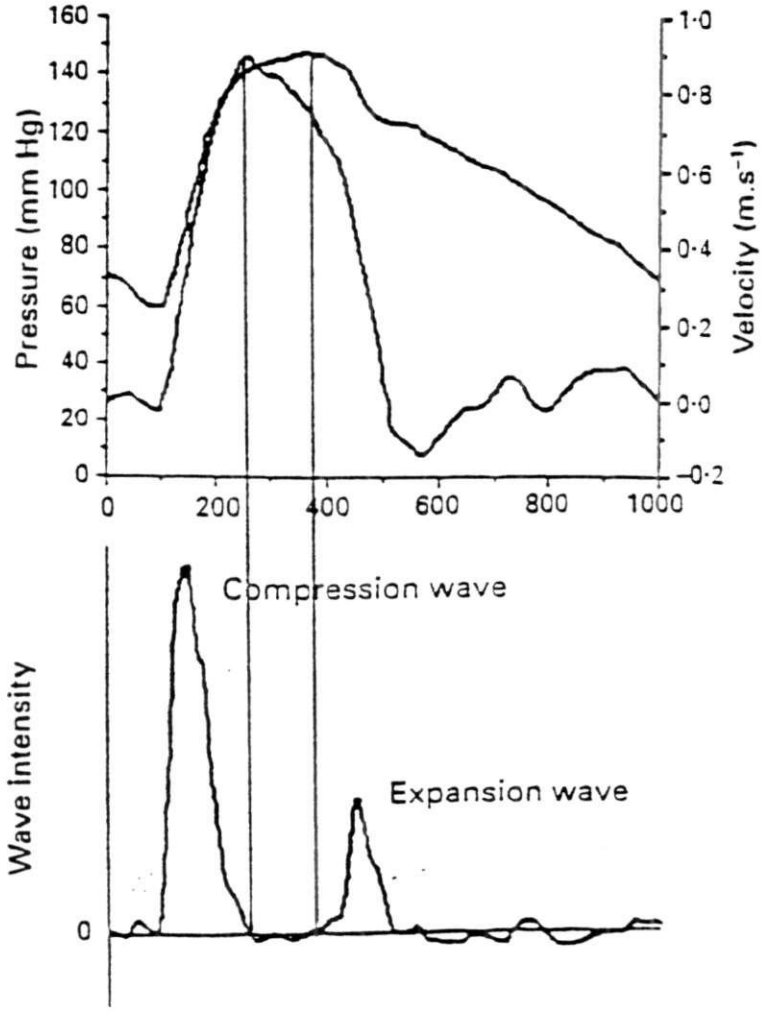

Figure 2.3: Wave-Intensity Analysis Applied to aortic Pressure – Flow

Figure 2.3 Wave-Intensity Analysis applied to aortic pressure and flow.

Wave-intensity determined for a normal human subject from the corresponding ascending aortic pressure and velocity. The wave-intensity pattern gives two positive peaks indicating that the LV generates compression and expansion waves in early and late systole. Note the absence of any wave-intensity activity in mid-systole which coincides with minimal net wave travel [43].

CHAPTER 3

EXPERIMENTAL METHODS

3.1 Animal Preparation

3.1.1 General Animal Care

All the study proposed in the thesis were performed on mongrel dogs (18- to 20-Kg) of either gender. Anesthesia was induced with sodium thiopental (25mg/kg iv) and maintained with fentanyl citrate (20-50mg/kg per hour, iv). The dogs were intubated and ventilated (70% nitrous oxide-30% oxygen mixture) using a constant-volume respirator (model 607, Harvard Apparatus Co Inc, Millis, Mass.) and a closed rebreathing system. Arterial P_{O2}, P_{CO2}, and pH were monitored and maintained at 90 to 120 mmHg, 30 to 40 mmHg, and 7.3 to 7.4, respectively, by adjustment of the tidal volume. Body temperature was maintained at 37.0 ± 0.5°C using a warming blanket and a heating lamp. A large-bore cannula was introduced into the external jugular vein for administration of fluids and the ECG was monitored.

3.1.2 Instrumentation

With the dog supine, a midline sternotomy was performed and the ventral surface of the pericardium was incised transversely along the base of the heart. Left ventricular pressure (P_{LV}) and aortic pressure (P_{Ao}) were measured using 8F catheter-tip manometers with fluid-filled reference lumens (model SPC-485A, Millar Instruments Inc, Houston Tex.) so that absolute values of pressure could be ascertained. Under fluoroscopic observation, from the left femoral artery, a JL2.5 Judkins catheter was advanced into the LCx through which a Doppler Flowire™ (Cardiometrics, Mountainview, Calif.) was introduced to measure LCx velocity

(U_{LCx}). LCx flow (Q_{LCx}) was measured using an ultrasonic flowprobe (Transonics, etc) placed at same location as the Doppler Flowwire. A pair of ultrasonic crystals was implanted in the anterior midwall of the LV to measure a circumferential segment length, L_{LV}. Pacing wires were attached to the right atrium for control of heart rate and to the right ventricular free wall and for control of heart rate and paired pacing to increase contractility [84]. Paired pacing, a classical method to increase myocardial contractility, produces postextrasystolic potentiation that constitutes an intrinsic augmentation of the contractile state of myocardium. The heart rate can be readily controlled when the paired stimuli are applied and the contractile state of myocardium is rapidly reversible. A pneumatic constrictor (In Vivo Metrics, Healdsburg, Calif.) was placed around the inferior vena cava. After cardiac instrumentation, the pericardium was reapproximated using single interrupted sutures [89]. All pressures were referenced to the mid-plane of the LV.

3.1 3 Coronary Pressure Measurement

Coronary pressure was recorded by a 2.5-F catheter-tip manometer (Millar) which was introduced into a 1.0- to 1.5-mm branch of the left circumflex coronary artery (LCx) and was advanced retrogradely 3 mm into the LCx coronary artery at the same location as velocity was measured, as shown in Figure 3.1. Because the LCx branch was too small to accommodate a catheter with a lumen, the absolute value of P_{LCx} could not be ascertained in the same manner as P_{LV}. However, in a series of 3 dogs, we recorded P_{LCx} using a fine plastic tube and a conventional

pressure transducer which demonstrated that P_{LCx} was equal to P_{Ao} during the mid-portion of diastole. Therefore, P_{LCx} was matched to P_{Ao}.

3.2 Data Collection

All the data, P_{LV}, P_{LCx}, P_{Ao}, U_{LCx}, L_{LV} ,Q_{LCx}, and the ECG, were recorded using a computer system (Sonometrics Corp., Ont.) with the respiratory machine tuned off at end-expiratory position. All the data were sampled at approximately 200 Hz.

3.3 Doppler Delay

WIA requires that the pressure and velocity should measured at the same location. Using a linear potentiometer, we measure the position of the plunger of a 5-ml syringe [39]. We compared the differentiated position signal to fluid velocity as measured using a Doppler Flowire™ (Cardiometrics, Mountainview, Calif.). We measured the Doppler delay in two ways:

1. Foot-to-foot method:
2. 50%-maximum method

A schematic diagram of foot-to-foot method (Method 1) and 50%-maximum method (Method 2) is shown in Figure 3.2. Forty-nine observations were analyzed. According to Method 1, the mean Doppler delay was 22.7 ± 0.6 ms and the median

was 22.9 ms. According to Method 2, the mean Doppler delay was 22.0 ± 0.8 ms and the median was 21.7 ms.

3.4 Data Analysis

All the data analysis was performed using specialized software (CVSOFT™, Odessa Computer Systems Ltd., Calgary, Alta.). On the basis of Doppler delay measurements and as confirmed by the manufacturer, we advanced all the Doppler Flowire™ data 20 ms in time.

WIA was applied to the study. We calculated dP and dU, the incremental difference in P_{LCx} and U_{LCx} during a sampling interval (0.005 s) from measured P_{LCx} and U_{LCx}. We calculated dP_+, dP_-, dI_{W+}, dI_{W-}, dI_W, I_{W+} and I_{W-} using equations **2.5**, **2.6**, **2.10**, **2.11**, **2.12**, **2.14**, and **2.15**, respectively. Wave speed *c* was calculated in each condition using equation **2.16**.

In order to assess contractility, the LV end-systolic pressure-length relation was calculated to obtain a length-based maximum elastance (E_{max}). Linear regression was applied to the end-systolic pressure-length points and the slope was defined as E_{max}.

Since *c* cannot be determined when both forward and backward waves are simultaneously present, *c* was calculated as the absolute value of $dP/\rho dU$ [75] at the beginning of systole, when we were confident that only a backward-going wave was

present. (c ranged between 5.3 and 7.9 m/s, values consistent with earlier measurements by other methods [3,29,86].)

3.4 Statistics

The Student's paired t test was used to identify statistically significant differences; a value of $P<0.05$ was considered significant.

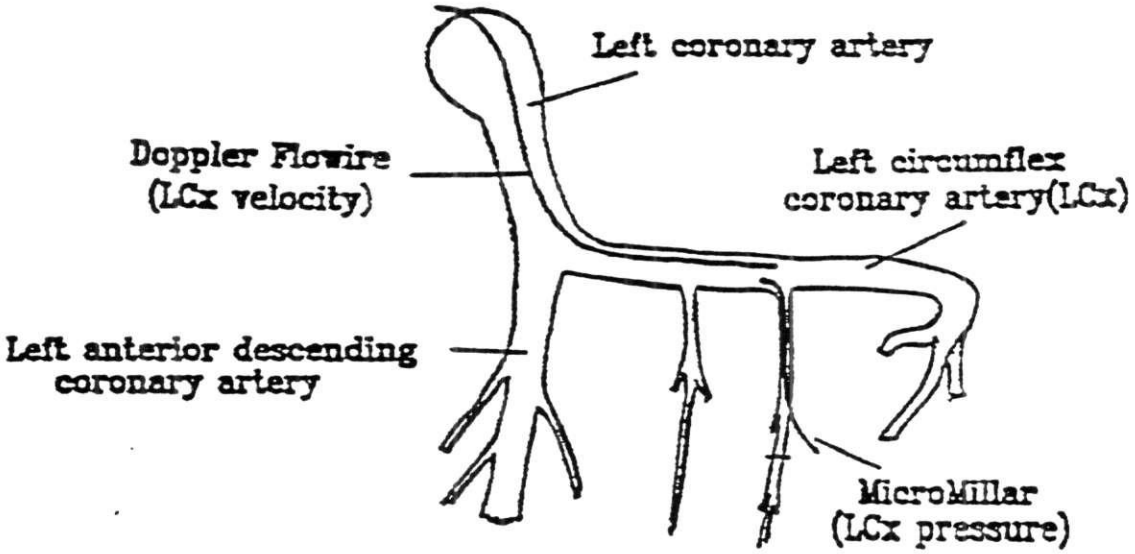

Figure 3.1 Schematic diagram of the placement of the pressure transducer and the Doppler Flowire within the distal left circumflex coronary.

Figure 3.1 Schematic diagram of the placement of the catheter-tip pressure transducer and the Doppler Flowire within the distal left circumflex coronary artery (LCx). Pressure and velocity were measured at same location

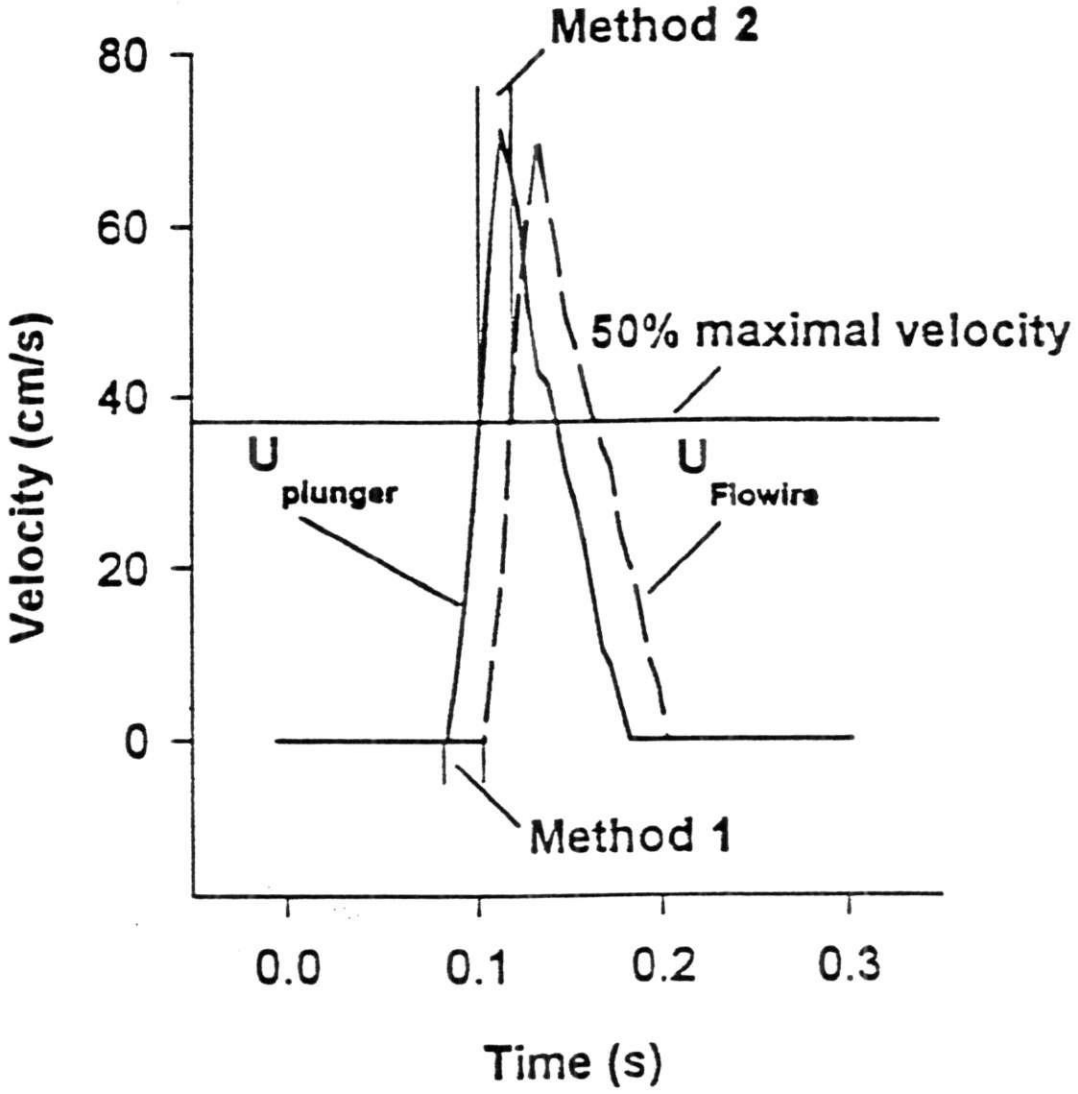

Figure 3.2 Determination of delay time of Doppler Flowire.

Figure 3.2 Determination of delay time of Doppler Flowire. A foot-to-foot method (method 1) and a 50% maximum method (method 2) are used to compare velocity of the syringe plunger ($U_{plunger}$) with velocity of the water ($U_{flowire}$).

CHAPTER 4

WAVE INTENSITY ANALYSIS IN THE CORONARY CIRCULATION

4.1 Introduction

Although aortic pressure is the main determinant of coronary artery pressure and flow, they are not simple functions of aortic pressure [52]. The coronary circulation is particularly complicated in that blood flows through the myocardium which, as it contracts, increasingly impedes flow. In the left ventricle, systolic coronary flow is small compared to diastolic flow [25-27,87,95], in contradistinction to those in the right ventricle in which maximal flow occurs during systole [7]. (That coronary systolic flow is small in large coronary arteries is related to the fact that flow reverses in the penetrating arteries [15], that subendocardial flow is retrograde [28], and that the capacitance of large epicardial coronary arteries is substantial [15].) The mechanisms by which LV contraction impedes left coronary blood flow have been studied for many years. The "vascular waterfall" [27] and the "intramyocardial pump" models [95] have been used to explain how increasing intramyocardial pressure impedes coronary blood flow during systole. Using a "time-varying elastance" model, Westerhof and his colleagues have explained how systolic flow is impeded by changes in extravascular stiffness that result from contraction of the fibers surrounding intramyocardial blood vessels [53].

These models explain the early-systolic decrease in coronary blood flow, but they do have limitations. First, they cannot explain the increase in coronary blood flow [15] that occurs after the initial minimum, in spite of the continuing increase in intramyocardial pressure and myocardial elastance. Second, because perfusion pressure was held constant in many previous studies, the results of those studies

might not apply to physiologic conditions when coronary pressure and flow vary throughout a cardiac cycle. Furthermore, coronary pressure and flow are determined by a) upstream aortic effects which are related to LV function and the properties of the systemic circulation and b) downstream microcirculatory effects, which are also related. Changes in LV function (e.g., changes in contractility) will affect both coronary perfusion pressure and myocardial compressive force and results from studies using constant perfusion pressure and maximal coronary vasodilation may over- or under-estimate the effects of contractility on coronary blood flow. Therefore, because of the need to identify and quantitate both upstream and downstream effects, we employed wave intensity analysis.

The purposes of the present study were 1) to clarify the dynamic pressure and velocity characteristics of the distal LV coronary circulation and 2) to provide a mechanistic explanation for acceleration and deceleration of coronary flow using WIA.

4.2 Methods

All the methods described in Chapter 3 are applied to this chapter. The following paragraphs describe the additional methods used in this chapter.

4.2.1 Animal Preparation

The study was performed on 10 18- to 20-kg mongrel dogs of either sex. Animal preparation and instrumentation are same as described in Chapter 3.

4.2.2 Protocols

After instrumentation and a 15- to 20-min stabilization interval, all the hemodynamic data (P_{LV}, P_{LCx}, P_{Ao}, U_{LCx}, and L_{LV}) were recorded while the heart was paced from the right atrium (Control 1). Then, a second set of control data (Control 2) was recorded while the heart was paced from the right ventricle using single stimuli. Finally, PP data were recorded while the heart was paced from the right ventricle using paired stimuli, to increase contractility [84]. Under Control 2 and PP conditions, caval constriction was applied to change left ventricular end-diastolic volume in order to obtain the end-systolic P_{LV} - L_{LV} relation, the slope of which (E_{max}) was taken as a measure of contractility. Individual hearts were paced at the same rate in Control 1, Control 2, and PP conditions. Between dogs, HR ranged from 85 to 100 min^{-1}.

4.2.3 Data Analysis

As a measure of the effect of LV systolic contraction on P_{LCx} , the pressure difference between P_{LCx} and P_{Ao} (ΔP_X) was measured at the P_{Ao}-P_{LV} crossover, as shown in Figure 4.1 and Figure 4.2. Also, I_W – and the values of dP_{LCx} /dt and dP_{Ao}/dt were measured during isovolumic contraction, the interval between end-diastole and the P_{Ao}-P_{LV} crossover, before and after contractility was increased by PP. The slopes, dP_{LCx} /dt and dP_{Ao}/dt, were calculated by taking the values of the slopes of straight-line segments drawn between the point of divergence [i.e., end-diastole] and the P_{Ao}-P_{LV} crossover.). Because it was difficult to ascertain the

absolute value of P_{LCx} and because the time derivatives are independent of the absolute values of pressure, dP_{LCx} /dt and dP_{Ao}/dt were compared to determine if paired pacing increased the divergence of P_{LCx} and P_{Ao}.

To determine the degree to which changes in dI_W governed changes in U_{LCx}, we measured the delay between the time during early ejection when dI_W crossed zero and the time at which U_{LCx} started to increase (i.e., when it stopped decreasing and started to increase; see Figure 4.1).

4.2.4 Statistics

Under each condition (Control 1, Control 2, and PP), 10 cardiac cycles were randomly selected and the average values obtained. Results from the 10 dogs were expressed as the mean $\pm$ SD. The Student's paired *t* test was used to identify statistically significant differences; a value of $P<0.05$ was considered significant.

4.3 Results

The figures that shown in this chapter are representative of all the preparations that were studied.

4.3.1 Net Wave Intensity.

Fig. 4.1 indicates the changes in coronary net wave intensity during a typical cardiac cycle. Between end-diastole and the moment that U_{LCx} reached a minimum, a backward-travelling compression wave was dominant, which was associated with

increasing P_{LCx} and decreasing U_{LCx}. Between the U_{LCx} minimum and the moment that P_{LCx} reaches a maximum, a forward-travelling compression wave was dominant, which was associated with a further increase in P_{LCx} and with increasing U_{LCx}. Later, during LV relaxation, a forward-travelling expansion wave developed and became dominant until the aortic valve closed at the incisura. This expansion wave was associated with decreases in both P_{LCx} and U_{LCx}. At the incisura, there was a brief, dominant, forward-travelling compression wave, which was associated with increases in both P_{LCx} and U_{LCx}. As LV relaxation continued, however, a backward-travelling expansion wave became dominant, which was associated with decreased P_{LCx} and increased U_{LCx}.

4.3.2 Intensity of Forward- and Backward-travelling Waves during LV Contraction

Figure 4.3 illustrates early systolic events in detail. The upper panel shows how P_{LCx} differs from P_{Ao}. Diastolic P_{Ao} fell monotonically until it was exceeded by P_{LV} (i.e., at the P_{Ao} - P_{LV} crossover). From mid-diastole, distal P_{LCx} was identical to P_{Ao} but, at the beginning of LV isovolumic contraction (i.e., at end-diastole), P_{LCx} stopped falling. Thereafter, it remained constant or began to increase somewhat but, in either case, it exceeded P_{Ao} until near the end of LV ejection.

As shown in the lower panel, we used WIA to clarify the mechanism that caused this difference between P_{LCx} and P_{Ao} . Immediately after LV end-diastole, a backward-travelling compression wave was generated and, after the opening of the

aortic valve, a forward-travelling compression wave. dI_{W-} started to increase (in absolute magnitude) after end-diastole, achieved its peak during early LV ejection, and returned to zero approximately at the time P_{LV} reached its peak. dI_{W+} started to increase at the beginning of ejection and, although it increased rapidly, its absolute magnitude did not become greater than that of dI_{W-} until after ~25 ms (i.e., the point at which dI_W became positive). It also returned to zero when P_{LV} reached its maximum value.

4.3.3 Effects of Paired Pacing

During Control 1, ΔP_X was 4.3 ± 2.5 mm Hg which doubled during paired pacing ($P < 0.0001$), an intervention which increased E_{max} (i.e., contractility) almost 3-fold (see Table 4.1). During the isovolumic contraction interval, dP_{Ao}/dt was –53.9 ± 19.5 mm Hg/s during Control 1 and did not change with paired pacing. dP_{LCx}/dt was 3.4 ± 4.4 during Control 1 ($P<0.0001$ vs dP_{Ao}/dt) and increased to 142 ± 25 mm Hg/s during paired pacing ($P < 0.0001$). As shown in the right-hand columns of Table 4.1, paired pacing increased the peak value of dI_{W-} by a factor of almost 3 and I_W by a factor of almost 4. There were no significant differences between data obtained during Control 1 and Control 2.

4.3.4 Intensity of Forward- and Backward-going Waves during LV Relaxation.

As illustrated in Figure 4.4, after the beginning of LV relaxation and the beginning of the decrease in P_{LCx}, forward and backward expansion waves began to

be generated. Typically, relaxation was characterized by triplets of both forward and backward waves. The forward and backward expansion waves in late systole were followed by forward and backward compression waves temporally related to aortic valve closure, after which there were paired forward and backward expansion waves.

4.4 Discussion

4.4.1 Apply WIA in Coronary Circulation

Among the systemic circulations, the LV coronary circulation is particularly complicated because both its driving force and impedance to flow are dynamic functions of contraction. LV contraction not only increases coronary perfusion pressure but several milliseconds earlier at end-diastole, begins to increase the compression of the microcirculation. LV relaxation not only decreases coronary perfusion pressure but decreases the compression of the microcirculation. Therefore, coronary blood velocity is determined by both upstream (aortic) and downstream (microcirculatory) events. Compared to previous approaches, the salient advantage of WIA is that it provides information about both upstream and downstream events in the time domain and therefore, on a beat-to-beat basis, provides direct information about the interaction of the upstream and downstream effects.

From the outset, it should be made clear that our WIA approach to waves in the arteries is fundamentally different from those approaches, which are based upon Fourier analysis. Fourier analysis is based upon the observation that any periodic waveform can be expressed as the summation of sinusoidal waves of different

frequencies (harmonics), each with the appropriate amplitude and phase. These sinusoidal wave trains are the fundamental basis of any Fourier technique, an archetypal example being the synthesis of speech from different sinusoidal tones.

An alternative approach to waves, WIA, is to consider the propagation of individual wave fronts characterized by a change in pressure, dP, and velocity, dU. An example of this type of wave is the "bore" seen in some river estuaries, notably the Severn, where a single wave front generated by the tide propagates up the river. It is convenient to consider small, infinitesimal wave fronts as the fundamental elements of our analysis since any finite waveform can be constructed from a sequence of individual wave fronts of the appropriate magnitude. For example, any wave form sampled at uniform intervals can be thought of as the summation of the changes between successive samples. This approach to the synthesis of a finite wave form has the advantage that it does not make any assumptions about periodicity and can therefore be applied to both transient and periodic wave forms. Beat-to-beat analysis is amenable to WIA whereas it is not if Fourier techniques are employed.

Wave intensity analysis was used to identify and quantitate upstream (aortic) and downstream (coronary microcirculatory) events and their interaction. dI_{w+} and dI_{w-} directly represent the respective effects of the upstream aorta and the downstream coronary microcirculation at any location. Therefore, when dI_w is positive ($dI_w > 0$), the forward-traveling wave (i.e., the aortic effect) is dominant; when dI_w is negative ($dI_w < 0$), the backward-traveling wave (i.e., the coronary microcirculatory effect) is dominant. dI_w represents the interaction of the aortic

effect with the coronary microcirculatory effect. If the values of dI_{w+} and dI_{w-} are similar or very small in magnitude, dI_w will be very small at that time and location.

The pressure change across a wave front can be positive, $dP > 0$ (which defines the wave as a compression wave), or negative, $dP < 0$ (which defines it as an expansion wave). Compression waves arise from pushing or blowing and they cause an increase of velocity in the direction of the wave. Expansion waves arise from pulling or sucking and they cause a decrease of velocity in the direction of the wave. If we define velocity to be positive in the direction of mean blood flow, a forward-going compression wave will accelerate the blood ($dU > 0$), whereas a backward-going compression wave will decelerate the blood ($dU < 0$). Similarly, a forward-going expansion wave will decelerate the blood ($dU < 0$), while a backward-going expansion wave will accelerate the blood ($dU > 0$). It may be helpful to think of blood flow in a coronary artery being manipulated by two "Maxwell demons," one at the arterial end of the artery and the other at the microcirculation end. The arterial demon could accelerate coronary blood flow by blowing into his end of the artery which would increase the pressure which would result in a forward-going compression wave. If, however, the microcirculation demon blew into his end of the artery it would similarly increase the pressure creating a backward-going compression which would decelerate the flow. If the microcirculation demon wanted to accelerate the flow, he would have to suck on the artery thereby decreasing the pressure. Note that simply measuring the change in pressure at some point in the artery cannot reveal the direction of travel of the wave front causing the change in pressure. To do this it is necessary to simultaneously measure the change in velocity. If, however, there are

simultaneous forward and backward waves, as is generally the case in the coronary arteries, then further analysis of the measured dP and dU are necessary to distinguish the properties of the two waves. WIA allows us to do this.

Between end-diastole and the moment that U_{LCx} reached a minimum, LV contraction generated a dominant, backward-travelling compression wave, which had the effect of increasing P_{LCx} and decreasing U_{LCx} (see Figure 4.1). (The compression of the vasculature resulted in a "pushing" effect that traveled backward, against the direction of blood flow.) Between the U_{LCx} minimum and the moment that P_{LCx} reaches a maximum, a forward-travelling compression wave generated by the increasing P_{Ao} became dominant, which continued to increase P_{LCx} further and to increase U_{LCx}. (The increase in aortic pressure resulted in a pushing effect that traveled forward, in the same direction as blood flow.) Later, as the LV began to relax and aortic pressure began to fall, a forward-travelling expansion wave developed and became dominant until the aortic valve closed at the incisura. (The decrease in aortic pressure resulted in a "pulling" effect that traveled forward, in the same direction as blood flow.) This expansion wave decreased both P_{LCx} and U_{LCx}. Aortic closure generated a brief, dominant, forward-travelling compression wave which increased both P_{LCx} and U_{LCx}. As LV relaxation continued, however, a backward-travelling expansion wave became dominant which decreased P_{LCx} and increased U_{LCx}. (Decreasing LV compression resulted in a pulling effect that traveled backward, against the direction of blood flow.)

4.4.2 Effects of LV Contraction on Coronary Blood Pressure and Velocity.

From high-fidelity measurements of aortic and distal coronary pressure, we have demonstrated that P_{LCx} is greater than P_{Ao} during LV isovolumic contraction, an observation that, to our knowledge, has not been reported previously. WIA identified an early-systolic backward-travelling compression wave (presumably generated by the contracting myocardium which causes retrograde subendocardial flow [15] and reverses flow in small penetrating branches [28].) which increased P_{LCx} and decreased U_{LCx}. When LV contractility was augmented by paired pacing, the changes in coronary pressure and the changes in the backward-travelling compression wave were consistent: ΔP_X, dP_{LCx}/dt, dI_{W-}, and I_{W-} all increased (Table 4.1). Westerhof and Sipkema and their colleagues related LV elastance to coronary flow impediment [53,55,56,108], we show (Chapter 5) that the peak intensity of the backward compression wave is directly related to systolic coronary flow reduction [104], and Suga and Sagawa equated increased myocardial elastance with increased contractility [88,101]. Thus, we conclude that paired pacing increased I_{W-} which caused the changes in P_{LCx}.

The same myocardial-compression mechanism that generates backward-going compression wave may account, in part, for the systolic pulsations in distal coronary pressure after a coronary artery has been occluded [95]. It may also account for retrograde systolic coronary flow [46] and the same phenomenon may be related to the observed systolic increase in epicardial coronary venous pressure [2]. During early systole, both the forward- and backward-going waves are compression waves and, as

such, both tend to increase P_{LCx}. We suggest that this may help to explain the fact that P_{LCx} continued to exceed P_{Ao} after the beginning of ejection.

Studies show that myocardial lymph pressure increases when LV pressure increased by aortic clamping [35,36]. It is a example of increase in myocardial elastance generates a bigger backward-compression wave which increases intramyocardial vessel pressure. Measurements of lymph pressure also show that, during diastole, lymph pressure is similar to left ventricular diastolic pressure. However, during systole, lymph pressure continues at approximately the same level, therefore much less than ventricular systolic pressure. These data have been interpreted to suggest that the systolic stiffened myocardium forms a more effective barrier between the ventricular lumen and the microvascular space [35].

Although dI_{W+} and dI_{W-} usefully represent the separate upstream aortic and downstream microcirculatory effects, dI_W (the net intensity) is important because it defines the balance of upstream and downstream forces and therefore determines whether the blood accelerates or decelerates. Because no forward wave was identified ($dI_{W+} = 0$) during isovolumic contraction, $dI_W = dI_{W-}$ and the unopposed backward compression wave decreased U_{LCx} and increased P_{LCx} (Figure 4.1). After the aortic valve opened, dI_{W+} began to increase and rapidly achieved an absolute magnitude almost as great as that of dI_{W-}. However, U_{LCx} began to increase only after approximately 25 ms. At that time when the intensity of the forward compression wave became greater than that of the backward compression wave (i.e., the upstream aortic pushing effect became greater than that from the downstream microcirculation), dI_W crossed 0 and became positive and U_{LCx} stopped decreasing

and began to increase. Thus, dI_W would seem to be an indicator of the "prevailing wind," and U_{LCx} changes immediately and accordingly.

After the beginning of ejection, dI_{W-} continued to increase (in absolute value). This may imply that vascular compression increased during later ejection when LV pressure continued to increase and LV volume decreased. Although increasing pressure and decreasing volume each would tend to increase dI_{W-}, the increase in dI_{W-} may be best predicted by the increase in elastance (the ratio of pressure to volume).

Using a special-purpose pressure generator, Kass and his collaborators have recently shown that systolic coronary flow is markedly augmented when pulse pressure is increased [80]. Although they have demonstrated that part of this increase is mediated by endothelium-dependent mechanisms [71,72], it seems clear that a substantial part of the increase must be attributed to a larger forward-going compression wave caused by the augmented pulse pressure.

For decades, investigators have attempted to understand the mechanism by which the contracting LV impedes its own blood supply and several models have been proposed to explain the decrease in coronary arterial flow in systole. The vascular waterfall model of Downey and Kirk [27] and the intramyocardial pump model of Spaan and his colleagues [95] have been used to explain how increasing intramyocardial pressure (itself closely related to LV pressure) impedes coronary flow. Using the time-varying elastance model, Westerhof and Sipkema and their colleagues have explained how systolic flow is impeded by changes in extravascular stiffness that result from contraction of the myocytes surrounding intramyocardial blood vessels

[53,55,56,108]. Although these models account for the early systolic decrease in flow, in themselves they do not account for the increase in flow that occurs during ejection when intramyocardial pressure and myocardial elastance both continue to increase. WIA appears to identify and quantitate both the forward- (dI_{W+}, due to aortic pressure) and backward-going waves (dI_{W-}, undoubtedly a function of intramyocardial pressure and elastance), and their net effect (dI_W) which governs velocity directly.

4.4.3 Effects of LV Relaxation on Coronary Blood Pressure and Velocity

Consistent with the concept that changes in LV elastance are similarly reflected in all of its cavities — luminal and vascular [53] — LV relaxation would appear to generate "aspirating forces" [112] which are manifest as forward- and backward-going expansion waves. With respect to the LV lumen, relaxation decelerates the column of aortic blood and decreases P_{Ao}; this effect is observed in the coronary artery as a forward expansion wave. With respect to the intramural LV vasculature, relaxation decreases microvascular compression; this effect is observed in the coronary artery as a backward expansion wave. Thus, in the coronary artery, the effects of LV relaxation are seen as both forward (via the aorta) and backward (via the vasculature) expansion waves. Closure of the aortic valve generated forward and backward compression waves which interrupted the expansion waves which preceded and followed them. (Presumably the forward compression wave generated by aortic

closure was primary and the backward compression wave generated by positive reflection from "closed-end" microcirculatory reflection sites was secondary.) Consistent with the fact that dI_W was positive during this interval (i.e., the forward compression wave was larger than the backward wave), velocity increased. After these paired forward and backward compression waves, relaxation again dominated as manifest by paired (i.e., forward and backward) expansion waves. Thus, LV relaxation seems to become manifest as triplets of forward and backward waves.

At the beginning of relaxation, the effects of both forward and backward expansion waves decreased coronary pressure, but they had different effects on coronary velocity: the forward expansion wave decreased blood velocity, but the backward expansion wave increased velocity. The net effect of these two waves determined flow velocity. Because $dI_{W+} > dI_{W-}$, $dI_W > 0$, the forward expansion wave dominated and coronary blood velocity decreased during this interval.

During the latter part of isovolumic relaxation, the relaxing myocardium generated a backward expansion wave that was greater than the forward wave. As the result, the dominant backward expansion wave ($dI_W < 0$, as shown in Fig. 6) increased coronary velocity and decreased coronary pressure. Although the early and late backward expansion waves were similar in magnitude, the late forward expansion wave was smaller, consistent with the fact that the closed aortic valve prevented aortic pressure from falling as fast as LV pressure. The phenomena of LV relaxation require further study.

4.5 Limitation

As described in Methods, because the caliber of the circumflex branch did not admit a catheter with a lumen, the absolute value of the high-fidelity P_{LCx} could not be ascertained by comparison to the output of an external transducer. Because dI_{W+} and dI_{W-} were negligible in the coronary artery during the interval preceding end-diastole, we assumed that P_{LCx} was equal to P_{Ao} and we therefore matched P_{LCx} to P_{Ao} at end-diastole. (This assumption was supported by measurements using an open catheter.) To the degree that this procedure was not accurate or appropriate, the values of ΔP_X might have been over- or under-estimated. However, the slopes of P_{Ao} and P_{LCx} do not depend upon the absolute values of P_{Ao} and P_{LCx} and the facts that the two pressures diverged and diverged more rapidly after paired pacing is unequivocal.

4.6 Conclusions

Wave-intensity analysis elucidates the dynamics of coronary blood flow and identifies and quantitates both the upstream (i.e., aortic) and downstream (i.e., coronary vascular) effects. During isovolumic contraction, distal coronary pressure exceeds aortic pressure and coronary velocity decreases, caused by a backward-going compression wave which is generated by increasing myocardial elastance, effects that are magnified when LV contractility is augmented by paired pacing. During LV relaxation, decreasing elastance appears to generate forward- (via the aorta) and backward-going (via the coronary vasculature) expansion waves. Thus, during contraction both upstream and downstream effects produce compression waves and, during relaxation, both upstream and downstream effects produce expansion waves. Coronary pressure and velocity depend on the balance of these effects.

Table 4.1 Coronary-Aortic Pressure Differences during Isovolumic Contraction and the Effects of Paired Pacing.

	E_{max} (mm Hg/mm)	dI_{W-} (W/m^2)	I_{W-} (J/m^2)	ΔP_X (mm Hg)	dP_{Ao}/dt (mm Hg/s)	dP_{LCx}/dt (mm Hg/s)
Control 1 (RA single pacing)	34.2±8.5	0.20±0.08	12.4±4.7	4.3±2.5	–53.9±19.5	3.4±4.4‡
Control 2 (RV single pacing)	36.6±10.6	0.23±0.09	13.9±5.2	4.5±2.0	–48.4±23.3	3.8±5.0‡
Paired pacing (RV)	93.6±20.7*	0.78±0.21*	46.8±12.8*	9.1±3.8*	–67.4±20.3	142.1±25.1*‡

Table 4.1 Values are means ± SD. E_{max}, the maximum, end-systolic value of elastance (i.e., contractility); dI_{W-}, the peak value of the intensity (power) of the backward-going compression wave; I_{W-}, the time-integral (energy) of the backward-going compression wave; ΔP_X, the difference between P_{LCx} and P_{Ao} at the P_{Ao}-P_{LV} crossover; P_{Ao}/dt and dP_{LCx}/dt, the slopes of P_{Ao} and P_{LCx} vs. time during isovolumic contraction;*, $P<0.0001$, paired pacing vs. Control 2; ‡, $P<0.0001$, dP_{Ao}/dt vs dP_{LCx}/dt; mean±SD.

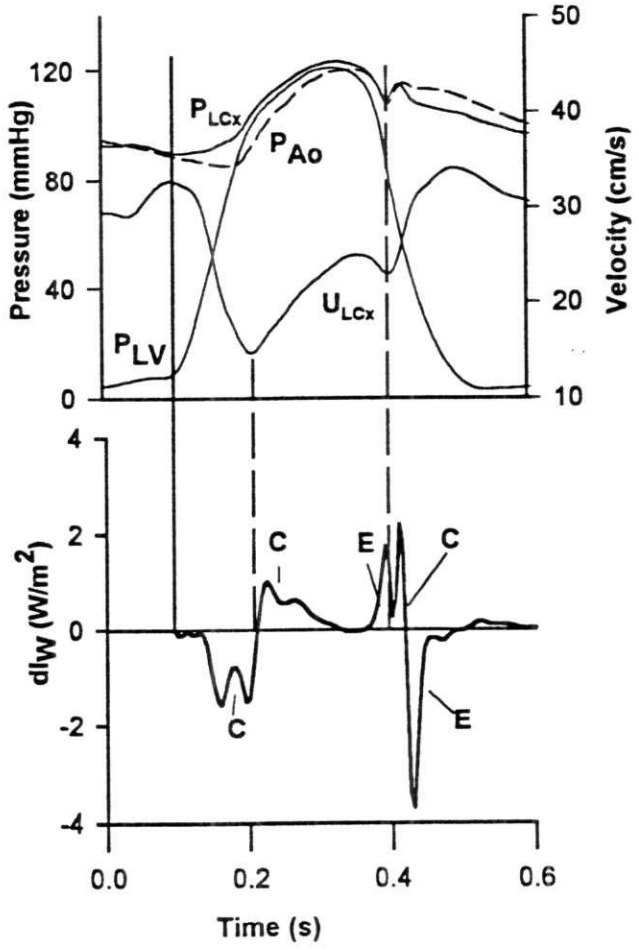

Figure 4.1 Net wave intensity during a representative cardiac cycle.

Figure 4.1 In the top panel are LV pressure (P_{LV}), aortic pressure (P_{Ao}, dashed line), coronary pressure (P_{LCx}), and coronary velocity (U_{LCx}) waveforms during a representative cardiac cycle. In the bottom panel is the net wave intensity (dI_W) waveform. "C" indicates a compression wave and "E," an expansion wave. The solid vertical line indicates end-diastole (ED) and the dashed vertical lines, the U_{LCx} minima.

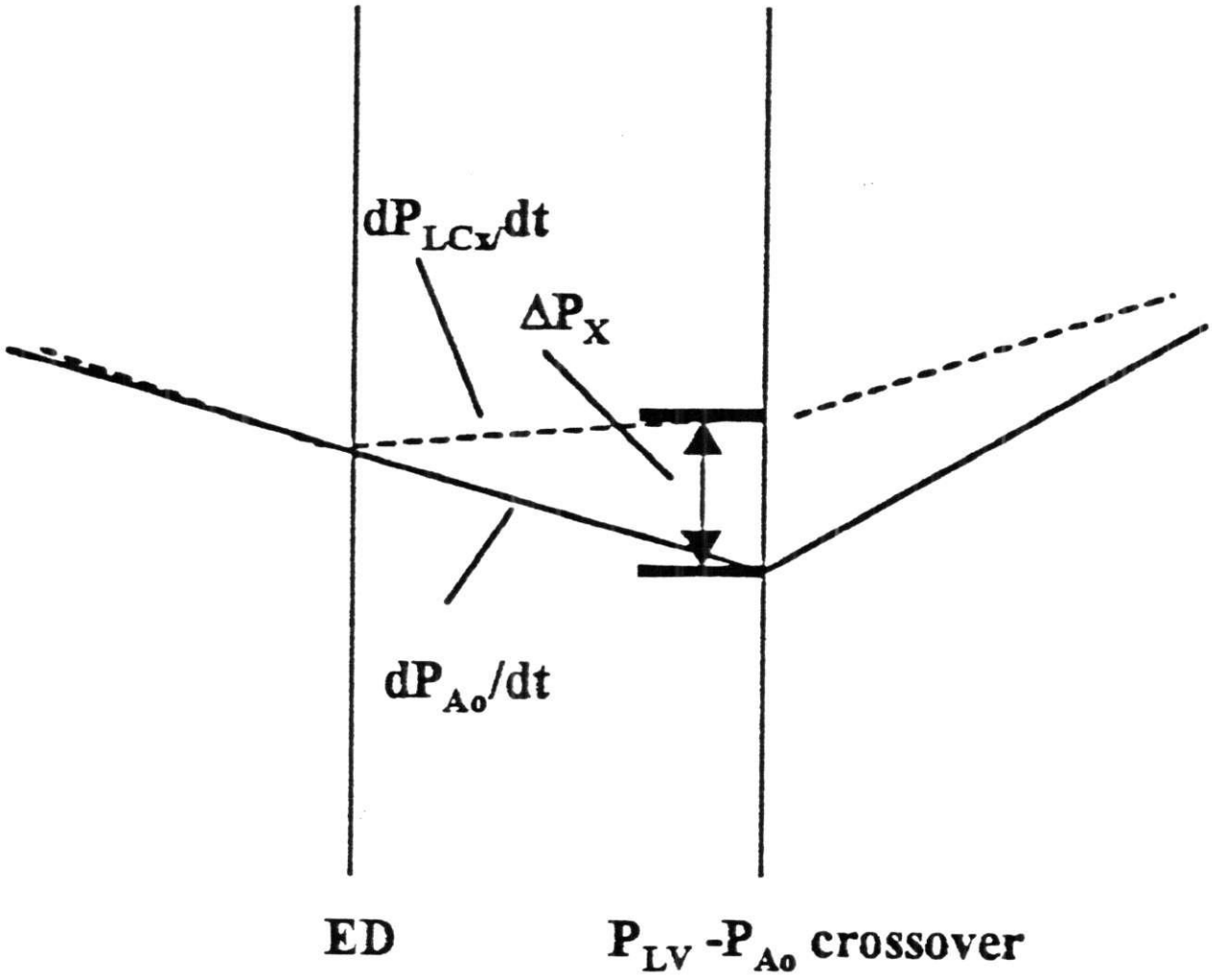

Figure 4.2 Illustration of the measurement of effects of LV contraction on coronary pressure

Figure 4.2. An idealized magnification of coronary pressure and aortic pressure during isovolumic contraction illustrates how we measured the effects of LV systolic contraction on coronary pressure. The two vertical lines indicate end-diastole (ED) and the moment at which the $P_{LV} - P_{Ao}$ crossover occurred; $)P_X$ indicates the P_{LCx} - P_{Ao} pressure difference at that moment. dP_{LCx}/dt and dP_{Ao}/dt represent the average slopes of P_{LCx} and P_{Ao} during the isovolumic interval.

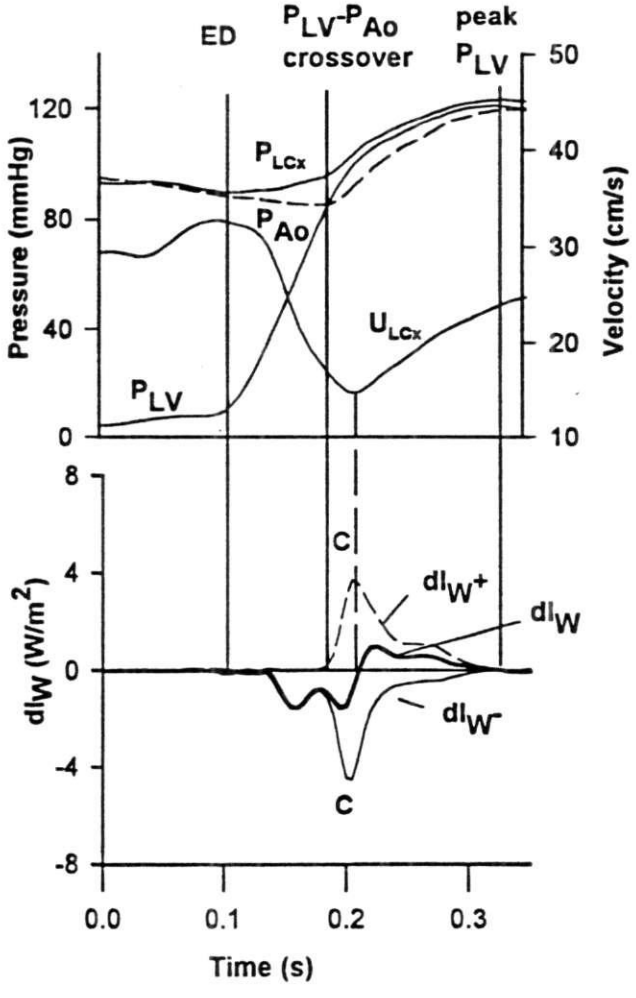

Figure 4.3 Forward-travelling and backward-travelling wave intensity during systole.

Figure 4.3. In the top panel are LV pressure (P_{LV}), aortic pressure (P_{Ao}, dashed line), coronary pressure (P_{LCx}), and coronary velocity (U_{LCx}) waveforms during an early systolic interval of a representative cardiac cycle. In the bottom panel are backward intensity (dI_{W-}, light solid line), forward intensity (dI_{W+}, dashed line), and net wave intensity (dI_W , heavy solid line) waveforms. "C" indicates a compression wave. Solid vertical lines indicate end-diastole (ED), the instant at which P_{LV} exceeds P_{Ao} (i.e., the P_{LV} - P_{Ao} crossover), and the time at which P_{LV} achieves its peak value. The dashed vertical line indicates the U_{LCx} minimum.

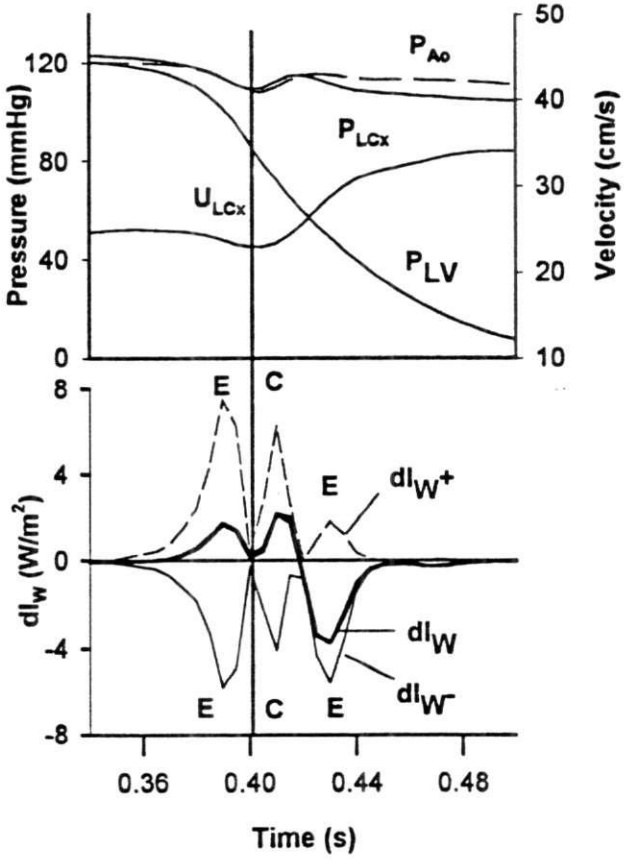

Figure 4 .4 Forward-travelling and backward-travelling wave intensity during diastole.

Figure 4.4 In the top panel are LV pressure (P_{LV}), aortic pressure (P_{Ao}, dashed line), coronary pressure (P_{LCx}), and coronary velocity (U_{LCx}) waveforms during early relaxation of a representative LV cycle. In the bottom panel are backward intensity (dI_{W-}, light solid line), forward intensity (dI_{W+}, dashed line), and net wave intensity (dI_W, heavy solid line). "E" indicates an expansion and "C," a compression wave.

CHAPTER 5

EFFECTS OF CORONARY TONE AND CONTRACTILITY ON CORONARY FLOW DYNAMICS

5.1 Introduction

The coronary circulation is particularly complicated because it passes through the beating heart. Coronary blood flow is a function of the pressure difference across the vascular bed (i.e., the coronary driving pressure) and the coronary resistance. Coronary driving pressure depends upon ventricular function. Coronary resistance has been discussed in terms of two components, one intrinsically vascular and one extravascular. Vascular resistance is determined by the tone of the smooth muscle in the coronary arterial wall, which is modulated by vasoactive agents. In addition, changes in ventricular performance change coronary vascular resistance via autoregulatory mechanisms. Extravascular resistance is generated by the contracting myocardium. Mechanical stresses in LV wall compress the coronary microcirculation during systole, increasing its resistance to blood flow [31]. Those mechanical stresses are increased by increased contractility, which has been shown to increase intramyocardial pressure and coronary systolic flow impediment in maximally dilated coronary arteries. [55,56]

In our previous study, we used WIA to study the effects of LV contraction and relaxation on the dynamics of coronary flow [103]. At the beginning of isovolumic contraction, a backward-travelling compression wave (BCW) is generated which continues until peak LV pressure is achieved and, when contractility is increased by paired pacing, the amplitude of this BCW increases. Thus, it seems clear that the BCW is caused by the systolic compression of coronary vessels and that it is directly responsible for the coronary systolic flow impediment. However, the effects of the

interaction of changing coronary tone and changing contractility on the BCW and the coronary systolic flow impediment are unknown.

Thus, the first goal of the present study was to define the effects of the early systolic BCW and coronary systolic flow impediment of changing coronary tone when contractility was held constant. We hypothesized that decreasing coronary tone would increase BCW and coronary systolic flow impediment, as vascular dilation could enhance the effects of myocardial compression. The second goal was to define the interaction of coronary tone and contractility when both were manipulated. We hypothesized that the greatest values of the BCW and coronary systolic flow impediment would be found when coronary tone was minimal and contractility was maximal.

5.2 Animal Preparation

The study was performed on 18 18- to 20-kg mongrel dogs of either sex. Animal preparation and instrumentation are same as described in Chapter 3.

5.3 Effects of Changing Coronary Tone on Coronary Flow Dynamics at Constant Contractility

5.3.1 Protocol

In 8 dogs, after instrumentation and a 15- to 20-min stabilization interval, all hemodynamic data (P_{LV}, P_{LCx}, P_{Ao}, U_{LCx}, Q_{LCx} and L_{LV}) were recorded

while the heart was paced from the right atrium (Control 1). A second set of control data (Control 2) was recorded while the heart was paced from the right ventricle using single stimuli. Coronary tone was then modified by LCx infusion (via the Judkins catheter) of vasodilators (adenosine and nitroglycerin) and a vasoconstrictor (phenylephrine). First, adenosine (0.022 mg/ml/min, 0.22 mg/ml/min, and 2.2 mg/ml/min), then phenylephrine (20 μg/ml/min, 60 μg/ml/min) and, finally, nitroglycerin (20 μg/ml/min, 60 μg/ml/min) were infused. After each drug effect was recorded, a 10-15 min recovery interval was allowed to elapse to regain hemodynamic stability. Immediately before a new drug was infused, all the hemodynamic data were recorded as a new control for that drug infusion. During each drug infusion and each individual control run, the inferior vena cava was constricted to describe a LV end-systolic pressure-length relation and to determine a length-based maximum elasticity (E_{max}) to assess contractility [88].

5.3.2 Data Analysis

WIA was used to identify and quantitate the effects of changing coronary tone on coronary systolic flow impediment (CSFI) at constant contractility. As described in detail in Chapter 2 and Chapter 3, we calculated dI_{W+}, dI_{W-}, dI_W, I_{W+}, I_{W-} and E_{max}.

As a measure of coronary arterial tone, coronary resistance (R_{LCx}) was calculated as the ratio of mean coronary pressure and flow:

$$R_{LCx} = \frac{\overline{P_{LCx}}}{\overline{Q_{LCx}}} \qquad (5.1)$$

The CSFI was calculated as the difference between the diastolic maximum and the systolic minimum of coronary flow [53]:

$$\mathbf{CSFI = Qmax - Qmin} \qquad (5.2)$$

The energy (I_{W-}) of the BCW were measured. As a measure of the effects of coronary tone on CSFI, only data from beats at same levels of contractility (E_{max}) were analyzed. In response to each vasoactive agent, R_{LCx}, CSFI and the value of I_{W-} were expressed as percentages of their control values (before the agent was infused). The percentage changes of CSFI were plotted as functions of the percentage changes in coronary tone and I_{W-}.

5.3.3 Statistics

Although there was no attempt to make observations in duplicate or to average groups of similar observations and provide measures of variability of the means, the regression analyses that were carried out describe the central tendency of the dependent variable as a function of one or more independent variables.

Regression analyses were performed using linear equations unless variance was significantly reduced (F statistic) by introducing non-linear equations, in which case exponential equations were chosen. The Student's paired *t* test was used to identify statistically significant differences; a value of $P<0.05$ was considered significant.

5.3.4 Results

Figure 5.1 demonstrates typical changes in coronary wave intensity during systole, before and after intracoronary infusion of vasodilators and a vasoconstrictor. Immediately after mitral valve closure, in each beat, a backward-travelling compression wave was generated and after the aortic valve had opened, a forward-travelling compression wave. dI_{W-} started to increase in magnitude after end-diastole, achieved its peak absolute magnitude during early LV ejection, and returned to zero approximately at the time P_{LV} reached its peak. dI_{W+} started to increase at the beginning of ejection and its absolute magnitude did not become greater than that of dI_{W-} until after ~30 ms. It also returned to zero when P_{LV} reached its maximum value. As shown, at a constant E_{max}, decreasing R_{LCx} by vasodilators (adenosine, nitroglycerin) increased the CSFI and the dI_{W-} and increasing R_{LCx} by a vasoconstrictor (phenylephrine) had the opposite effects.

We plotted the changes of CSFI vs. the changes of R_{LCx} in Figure 5.2 and found that CSFI was inversely related to R_{LCx} ($R=-0.91$, $p<0.001$). When R_{LCx} was increased by 15%, CSFI decreased by 25% and, when R_{LCx} was decreased by 15%, CSFI increased by 30%. The changes of I_{W-} vs. the changes of R_{LCx} were plotted in Figure 5.3. It shows that, when E_{max} remained constant, increasing R_{LCx} decreased I_{W-} ($R=-0.91$, $p<0.001$). When R_{LCx} was increased by 15%, I_{W-} decreased by about 35%. However, when R_{LCx} was decreased by 15%, I_{W-} was increased by 70%. As CSFI and I_{W-} were both inversely related to R_{LCx}, CSFI was proportional to I_{W-} (Figure 5.4; $R=0.92$, $p<0.001$).

5.4 Effects of Coronary Tone on Coronary Flow Dynamics at varied Contractility

5.4.1 Protocol

In 10 dogs, in addition to the procedures performed during the protocol which is described in 5.3.1, paired pacing was instituted before and after each drug infusion. In each state, the inferior vena cava was constricted to assess contractility.

5.4.2 Data Analysis

In addition to the data analysis described in 5.3.2, in order to define the combined effects of changing coronary tone and changing contractility on CSFI, CSFI and I_{W-} were plotted as functions of E_{max} and R_{LCx} in 3-D meshed plots. Only the first beat of paired-pacing data was used to minimize the contribution of secondary metabolic changes.

5.4.3 Results

Figure 5.5 illustrates the increases in I_{W-} and CSFI due to increased E_{max} (caused by ventricular paired pacing). Increasing E_{max} increased CSFI as well as dI_{W-} and I_{W-}.

We plotted CSFI as a function of both R_{LCx} and E_{max} (Figure 5.6). It shows that, when E_{max} was low, decreasing R_{LCx} increased CSFI slightly but not so much as when E_{max} was high. When R_{LCx} was high, increasing E_{max} increased CSFI but not so

much as when R_{LCx} was low. Again, when we plotted I_{W-} as a function of both R_{LCx} and E_{max} (Figure 5.7), a surface of a similar shape was seen. It suggests that, when E_{max} is constant, reducing R_{LCx} increases I_{W-}; when R_{LCx} is constant, I_{W-} is contractility-dependent; I_{W-} is greatest at the highest values of E_{max} and the lowest values of R_{LCx}. Statistical analysis indicated that I_{W-} varied inversely and linearly with E_{max} but inversely and non-linearly with R_{LCx} (i.e., variance was reduced when an exponential relation was selected).

5.5 Discussion

We have used wave-intensity analysis to clarify the mechanism by which changes in coronary vascular tone and contractility affect the magnitude of the BCW and its impeding effect on coronary blood flow as assessed using wave intensity analysis. As anticipated by the results of the previous study described in Chapter 4, we here find that increasing contractility increases both the BCW and the CSFI. In addition, we here find that decreasing coronary tone also increases both the BCW and the CSFI.

In order to study the effects of coronary vascular tone on CSFI, vasodilators and a constrictor were infused into the left circumflex coronary artery to change vascular tone. Infusions of vasodilators increased CSFI by increasing the maximum diastolic flow more than the minimum systolic flow. Infusion of a vasoconstrictor decreased CSFI by decreasing the maximum diastolic flow more than the minimum systolic flow.

Because changing coronary blood flow by vasoconstrictors and vasodilators may also alter contractility, we very carefully assessed contractility using E_{max} from LV pressure-length loop and selected pairs of beats with same end-diastolic pressure and E_{max}, before and after the vasoactive agents were infused. At constant contractility, when coronary vascular tone was decreased by vasodilators, CSFI was increased and, when coronary tone was increased by vasoconstrictors, CSFI was decreased; thus, changes in CSFI were inversely related to the changes of coronary vascular tone. This implies that the dilated coronary system increases the sensitivity to response to myocardium contraction. In the other words, the same extravascular force would seem to cause a larger coronary flow reduction when the coronary vessels are dilated. Increased coronary tone minimizes the coronary flow reduction caused by extravascular compression

These effects on CSFI are related to the fact that it is a measure of absolute flow reduction. Vasodilators increased both diastolic and systolic flow in approximately the same proportion; thus it was inevitable that the difference should increase in absolute magnitude. The opposite was true of the effect of vasoconstriction. Compared with the other group's study [1], it shows that increasing contractility mainly increases maximum diastolic flow, but has little effect on minimum systolic flow. This different result may due to that they used the maximum dilated coronary artery model.

Under normal physiologic conditions, coronary vascular tone and contractility may change, spontaneously and independently. To assess the effects of changing contractility on CSFI at different levels of coronary tone, paired pacing was used to

increase contractility before and after intracoronary infusions of vasoactive agents. In order to avoid complicating the effect of the change in contractility with the additive effect of the resultant metabolic vasodilatation, we selected only the first beat of the paired-pacing run for analysis. Increased contractility and decreased coronary vascular tone interact to increase the magnitude of the BCW and the CSFI.

Figure 5.8 is a schematic diagram of the possible mechanisms by which, at any level of contractility, decreasing coronary tone might increase the BCW and the CSFI. Spaan's concept [94] of the myocardium compressing the compliant coronary vasculature implies that coupling might be improved by vasodilatation. This improved coupling might result in a larger BCW "at its source," as expressed diagrammatically by the larger downward-pointing arrow in the upper, right-hand panel. Thus, in the absence of a change in the attenuation of the "original" BCW, a larger BCW will be measured in the coronary artery (e.g., the left circumflex). Secondly, vasodilation might reduce the attenuation that the BCW sustains before it reaches the coronary artery. This mechanism is diagrammed in the lower panels. Obviously, these mechanisms might exist in some combination. In the present study, vasodilators adenosine and nitroglycerin were used to change coronary tone which act in resistance vessels and conduit vessels in the coronary circulation respectively. Wave intensity analysis shows that the waveform of backward-travelling compression wave during systole after adenosine and nitroglycerin infusion is different as shown in Figure 5.1. The effect of adenosine infusion produces a big amplitude change in backward intensity, while nitroglycerin infusion produces a relatively longer duration but smaller in amplitude change of backward intensity. This may imply that the

effects of vasodilatation in coronary microcirculation achieved by adenosine is mainly acting through the coupling mechanism; while the effects of vasodilatation in coronary conduit vessel achieved by nitroglycerin is mainly acting through the resistance mechanism. New experiments need to be designed to determine which mechanism is more important.

Spaan et al has shown that the sensitivity of lymph pressure to a change in LV pressure in much larger during diastole than during systole [35]. It implies that the increased elastance of myocardium "protects" intramyocardial lymph vessels from the effects of LV pressure. This concept is somewhat similar to our interpretation of the effects of vasoconstrictors: vasoconstrictors (increased elastance of coronary vessel) decrease the effects of myocardial contraction on coronary flow.

The magnitude of the BCW (and thus CSFI) has been shown to represent the interaction of coronary tone and contractility. When contractility is constant, changes in the BCW reflect changes in coronary tone and, when coronary vascular tone is constant, changes in the BCW reflect changes in contractility. When both contractility and coronary vascular tone change, changes in the BCW represent the combined effects.

Coronary tone and LV contractility both play important roles in modulating coronary blood flow. A better understanding of the mechanisms whereby the coronary microcirculation and LV contractility interact to modulate coronary flow dynamics may ultimately be helpful for patient management. β-blocker therapy has been shown to be effective in treating ischemic heart disease and the results of this

study – that decreasing contractility may increase systolic blood flow – may provide another partial rationale for their use.

5.6 Conclusions

Our data suggest that both contractility and coronary vascular tone modulate the backward-going compression wave and, thus, the coronary systolic flow. Coronary vascular tone increases the sensitivity of the coronary microcirculation to myocardial compression, which is manifested as a larger coronary BCW. The dilated coronary microcirculation might be better coupled to the myocardium and, thus, more susceptible to compression and/or the arterial attenuation of the BCW might be decreased. Increasing contractility increases the BCW and the coronary systolic flow impediment.

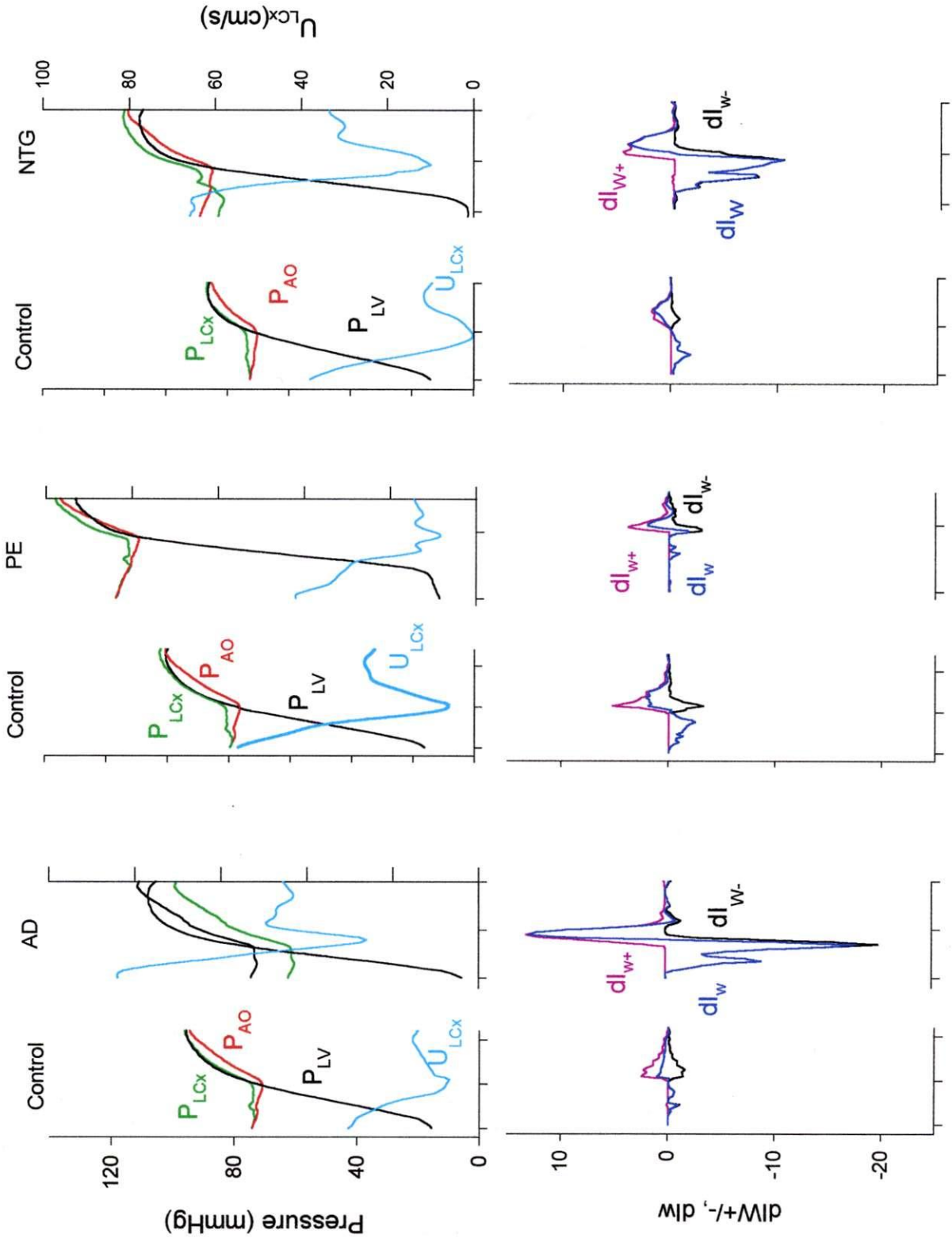

Figure 5.1 Changes in early systolic coronary wave intensity due to infusion of vasodilators and vasoconstrictor

Figure 5.1. Changes in early systolic coronary wave intensity due to infusions of adenosine (AD), phenylephrine (PE), and nitroglycerin (NG). The upper panels show left circumflex (P_{LCx}; green), left ventricular (P_{LV}; black), and aortic (P_{Ao}; red) pressures and left circumflex blood velocity (U_{LCx}; light blue); the lower panels show the intensity of the forward- (dI_{W+}; positive values in pink) and backward-travelling waves (dI_{W-}; negative values in black) and the net intensity (dI_W; blue). Note that the vasodilators increased and the vasoconstrictor decreased dI_{W-}.

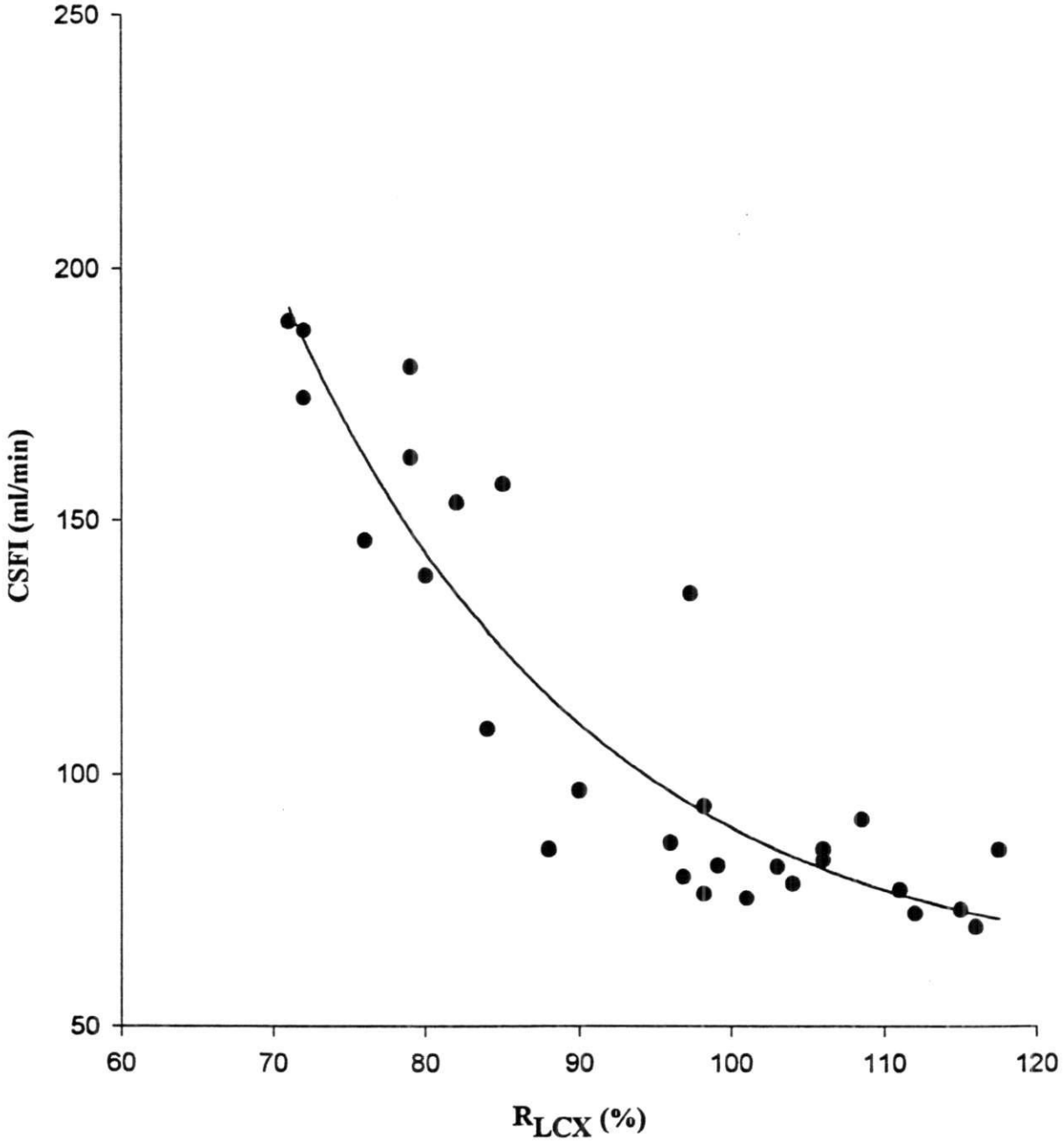

Figure 5.2 Changes in coronary systolic flow impediment as a function of the change in coronary tone.

Figure 5.2. Changes in coronary systolic flow impediment as a function of the changes in coronary tone (R_{LCx}) at constant contractility. $CSFI = 58.8 + 4797\exp^{(-0.05RLCx)}$; $R = 0.92$, $p < 0.001$.

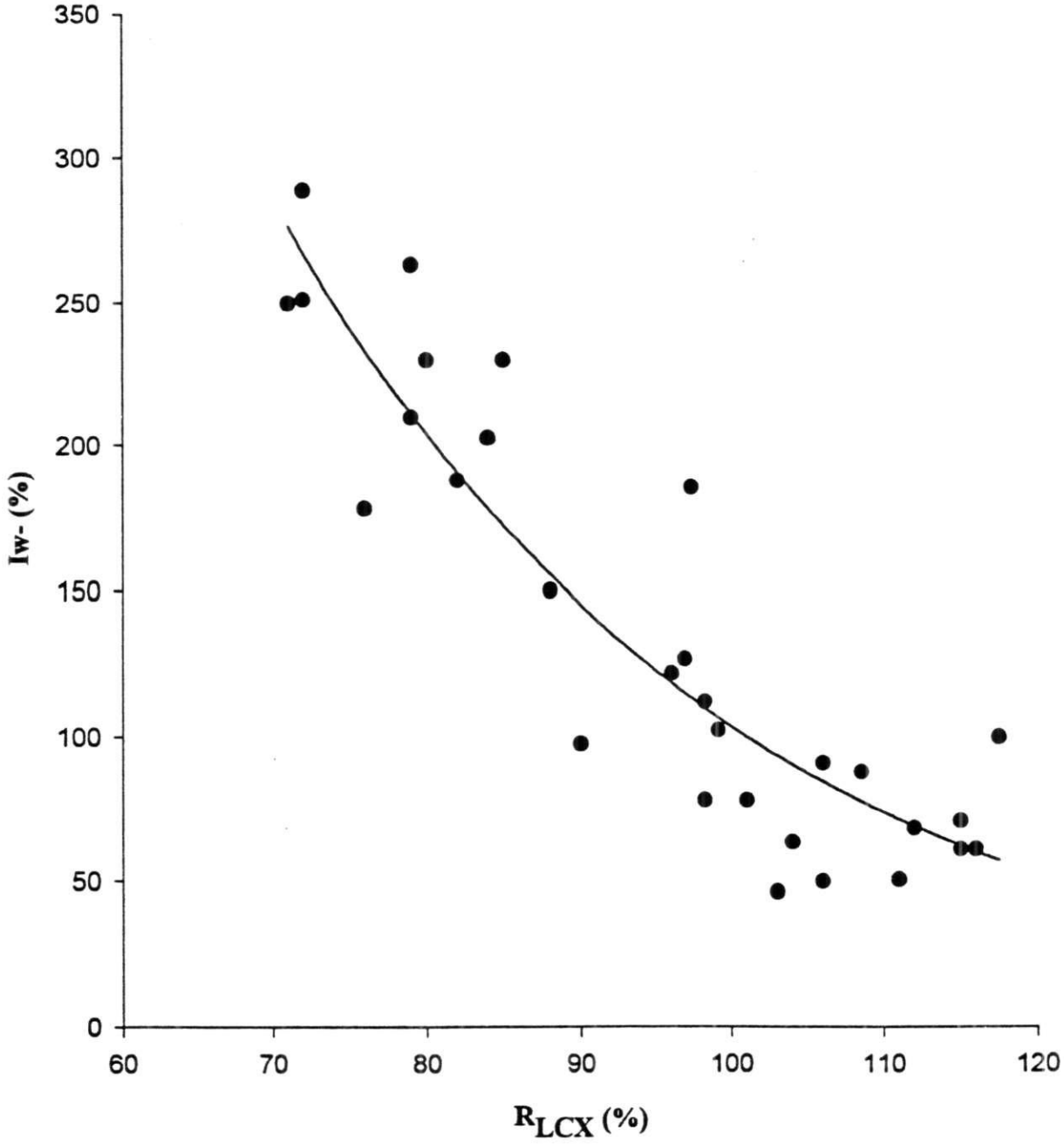

Figure 5.3 Changes in the energy of the backward-travelling compression wave as a function of changes in coronary tone at constant contractility

Figure 5.3. Changes in the energy (I_{w-}) of the backward-travelling compression wave as a function of changes in coronary tone (R_{LCx}) at constant contractility. $Iw- = 3060\exp^{(-0.03RLCx)}$; $R = 0.91$, $p<0.001$.

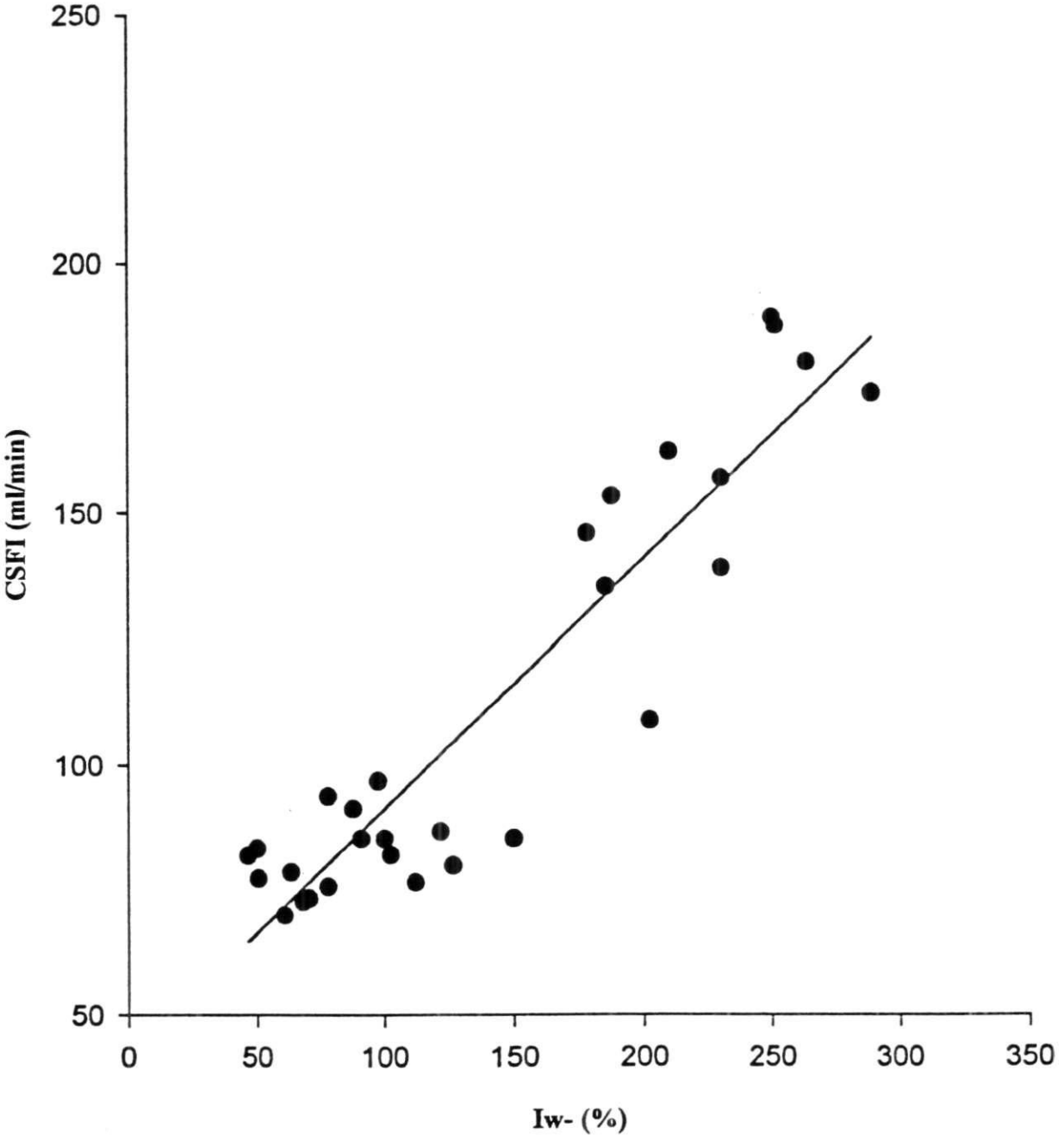

Figure 5.4 Changes in coronary systolic flow impediment as a function of the changes in the energy of the backward-travelling compression wave at contant contractility.

Figure 5.4. Changes in coronary systolic flow impediment as a function of the changes in the energy (I_{W-}) of the backward-going compression wave at constant contractility. CSFI = 41.6+ 0.5Iw-; R = 0.92, p< 0.001

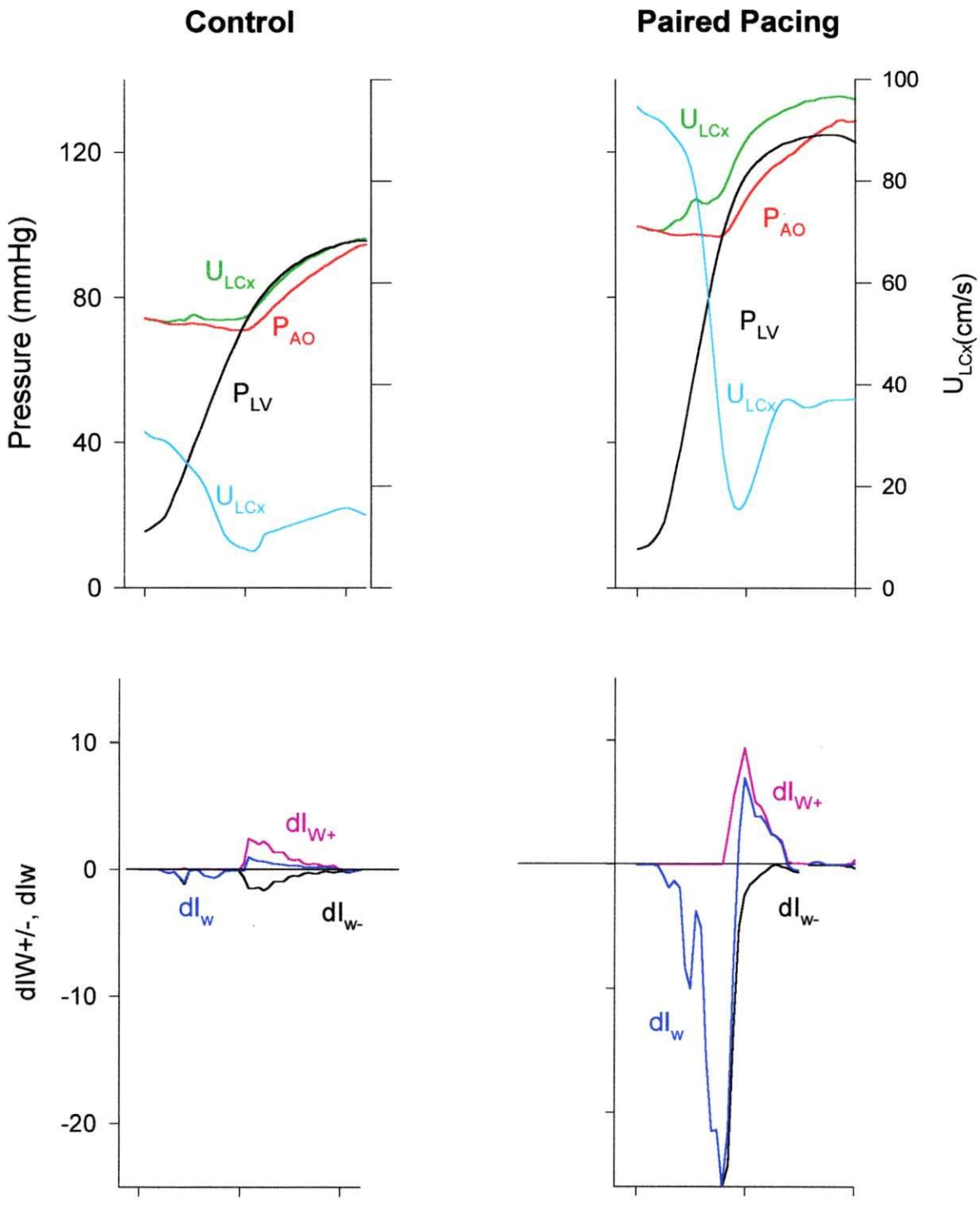

Figure 5.5 Changes in early systolic coronary wave intensity due to increased contractility.

Figure 5.5. Changes in early systolic coronary wave intensity due to increased contractility (paired pacing). Abbreviations and color conventions as in Figure 5. 1.

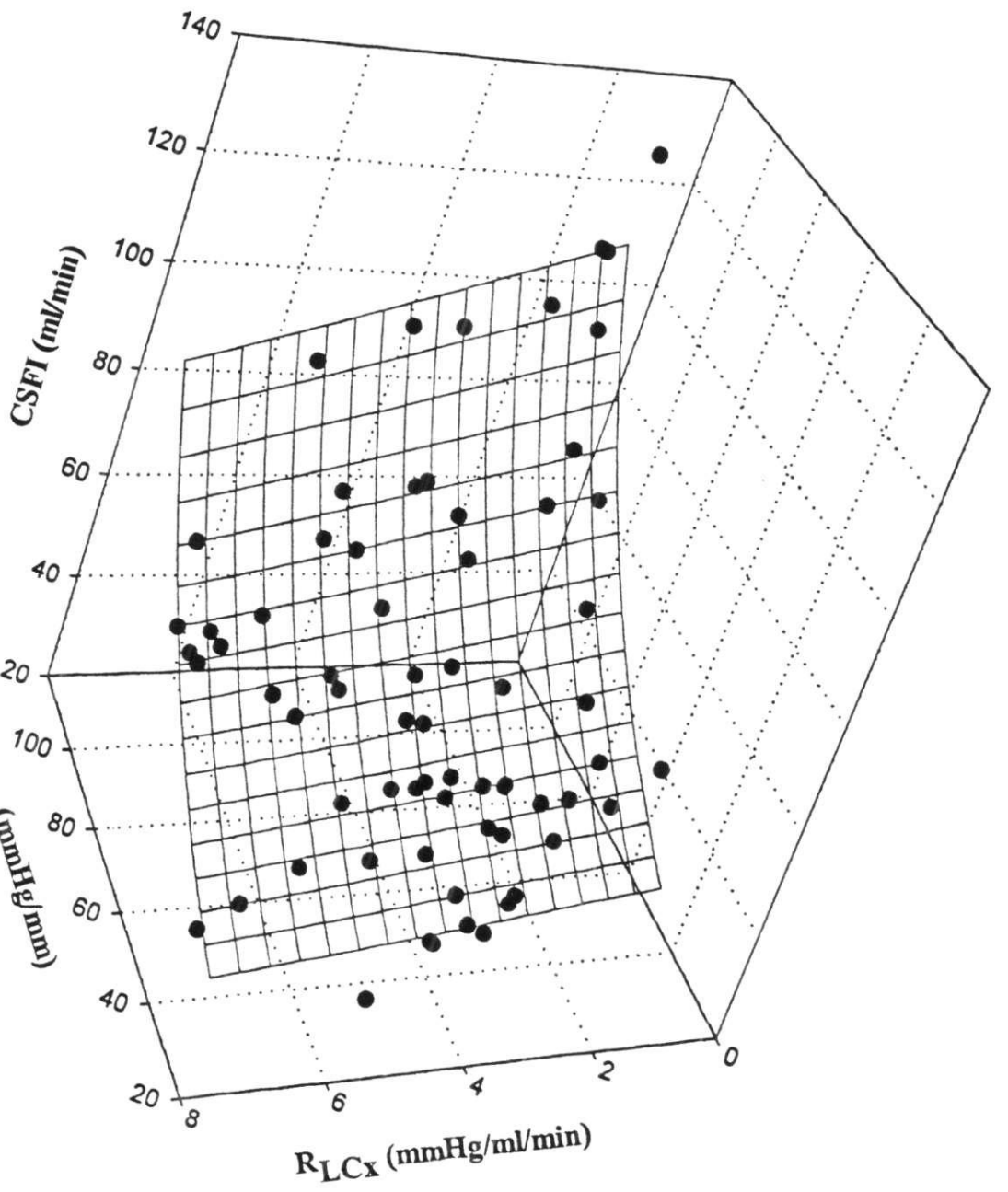

Figure 5.6 3D meshed plot of CSFI as a function of contractility and coronary tone

Figure 5.6. 3-D meshed plot of coronary systolic flow impediment as a function of E_{max} (contractility) and R_{LCx} (coronary tone). There is an inverse relationship between CSFI and both contractility and coronary tone. Pooled data from 10 dogs. $CSFI = 519/[1+\{(E_{max}-206.3)/62.05\}^2]*[1+\{(R_{LCx}+12.7/23.7\}^2]$; $R = 0.88$, $p<0.001$.

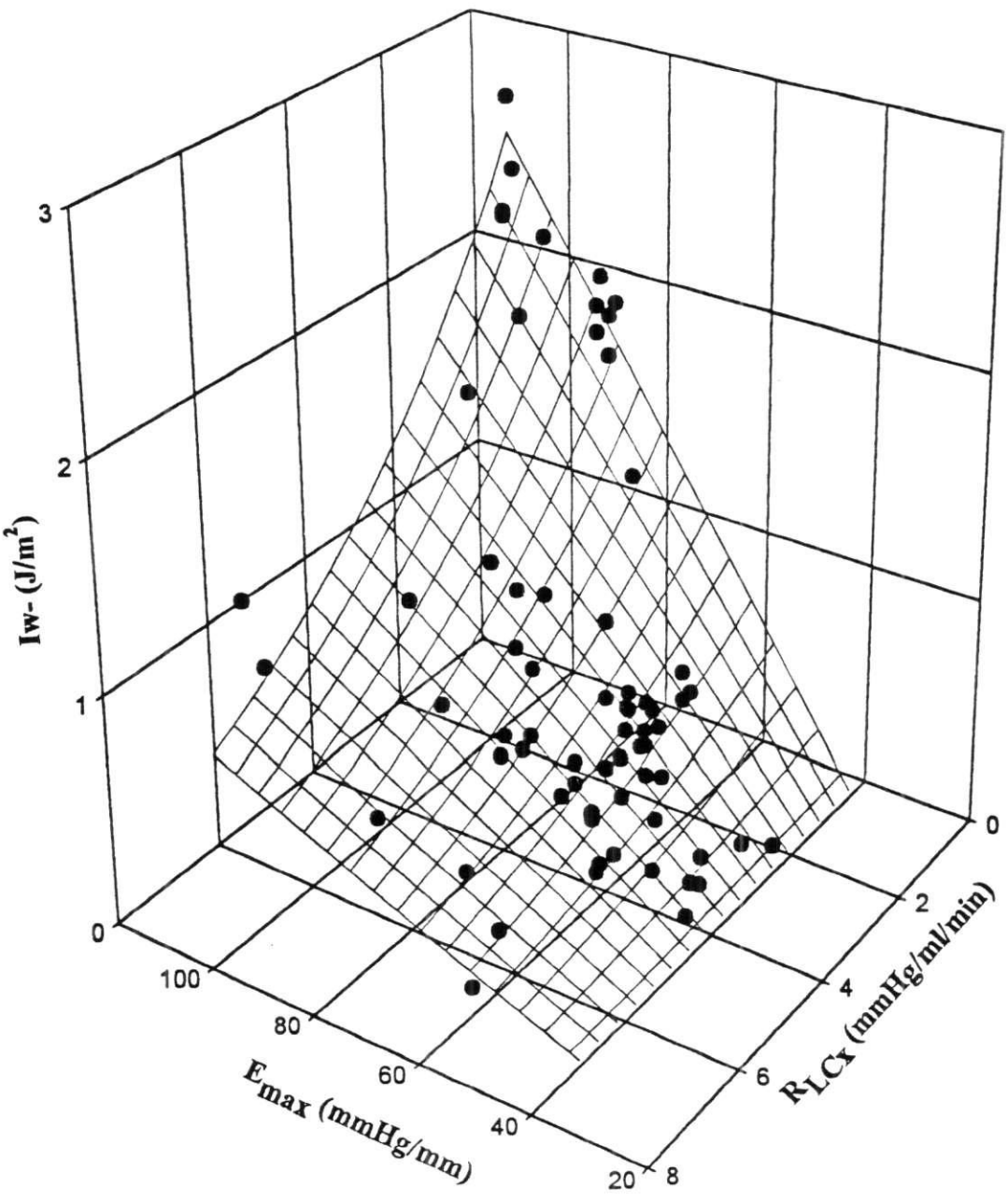

Figure 5.7 3D meshed plot of the backward-travelling compression wave as a function of contractility and coronary tone

Figure. 5.7 3-D meshed plot of the energy (I_{W-}) of the systolic backward-going compression wave as a function of E_{max} (contractility) and R_{LCx} (coronary tone). There is an inverse relationship between the energy of the BCW and both contractility and coronary tone. Pooled data from 10 dogs. $I_{W-} = 0.528e^{-0.206R_{LCX}}(0.069E_{max}-2.7)$; $R=0.94$, $p<0.001$.

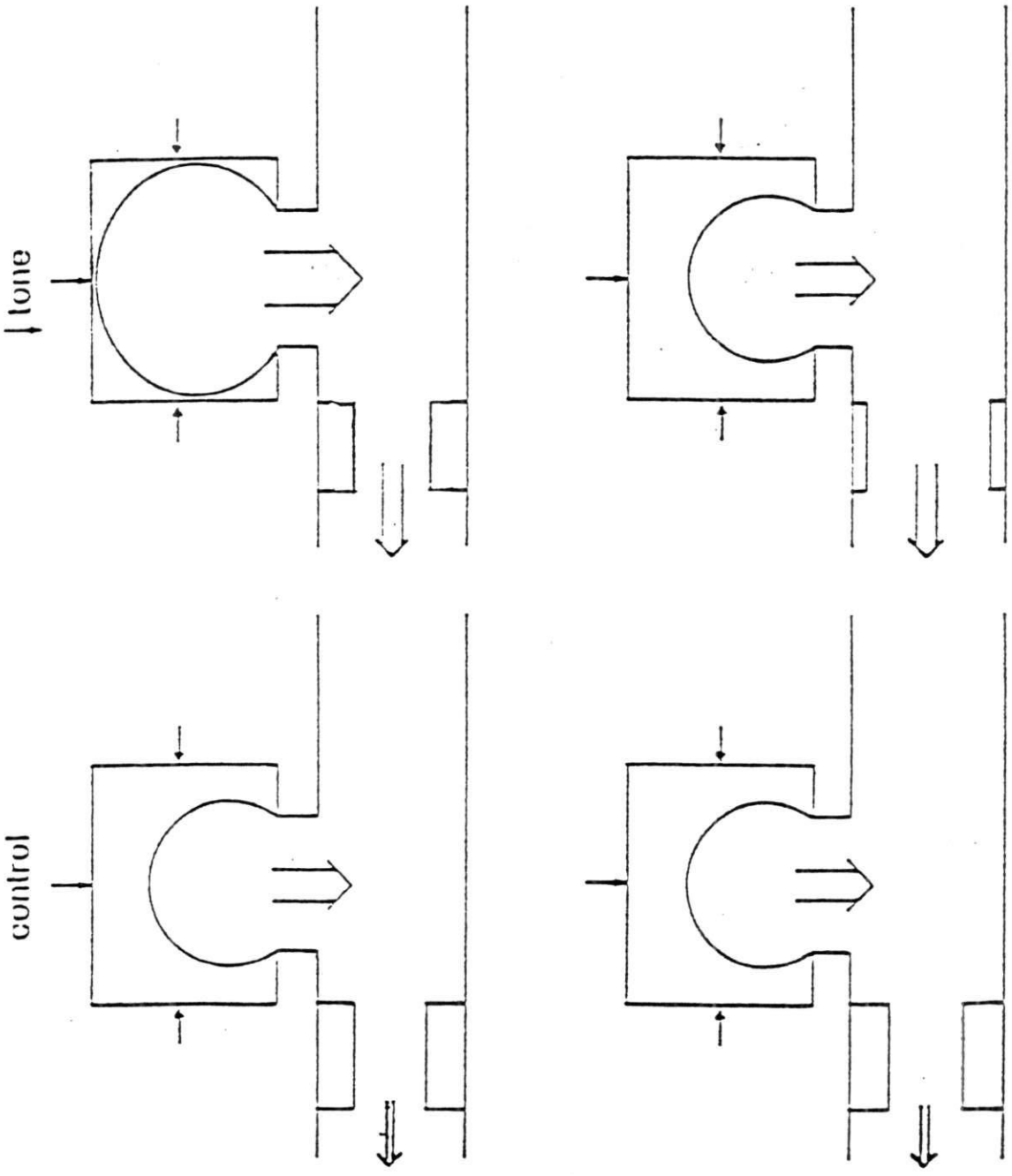

Figure 5.8 Schematic diagram of possible mechanisms of how change on contractility and coronary tone modulate the magnitude of the BCW and the CSFI.

Figure 5.8 Schematic diagram of possible mechanisms by which, at any level of contractility, decreases in coronary tone might increase the magnitude of the BCW and, thus, the CSFI. As shown in the top panels, a decrease in tone (right panel) might enhance the coupling between the coronary vessels and the surrounding musculature; the result would be a larger BCW "at its source," as suggested by the wider, downward-pointing arrow. Secondly, as shown in the bottom panels, a decrease in tone might reduce the attenuation of the original BCW such that the observed BCW is larger.

CHAPTER 6

SUMMARY AND CONCLUSIONS

While the heart pumps blood to serve the whole body, the heart muscle itself must be perfused. Because most of the coronary blood vessels are embedded in the myocardium, they are squeezed by myocardium with each contraction. Coronary systolic flow impediment is directly related to myocardial contraction. The interaction between myocardial contraction and coronary vascular tone dominates coronary blood flow. Thus, coronary blood flow is determined by both upstream aortic effects and downstream coronary microcirculatory effects. This thesis focuses on the effects of contractility and coronary tone on coronary flow dynamics using wave intensity analysis, which can separate downstream events (dI_W-) from upstream events (dI_W+) and provide information regarding their interaction (dI_W).

The mechanisms by which left ventricular contraction impedes left coronary blood flow have been explained, in the past, by the " vascular waterfall " mode, the "intramyocardial pump" model, and the "time-varying elastance" model. Many of these studies were done with artificial constraints: 1) Because the coronary arteries were usually cannulated, the perfusion pressure was held constant and independent of left ventricular pressure and work. 2) Because many studies used maximally vasodilated coronary vessels, it remained unclear how left ventricular contraction affects coronary flow with vascular tone present. The present study using wave intensity analysis does not require coronary arterial cannulation and obtains results beat by beat.

A Doppler Flowire was used in this study to measure coronary blood velocity directly. In Chapter 3, it is shown that the velocity signal measured by the Doppler

Flowire was delayed by about 20ms. Therefore, before wave intensity was calculated, it was necessary to advance the velocity signal by 20 ms.

In Chapter 4 wave intensity analysis was used to identify and quantitate upstream aortic and downstream coronary microcirculatory events and their interaction. It was shown that myocardial contraction generates a backward-travelling compression wave, which is responsible for the increase in coronary pressure and the decrease in coronary flow during early systole. Coronary pressure becomes greater than aortic pressure as aortic pressure continues to decrease. When left ventricular contractility was augmented by paired pacing, coronary pressure increased, consistent with the increase in the backward-travelling compression wave. It was also demonstrated that the backward-travelling compression wave is directly related to the coronary systolic flow impediment. Thus, we conclude that during isovolumic contraction, a backward-travelling compression wave generated by the contracting myocardium causes coronary pressure to exceed aortic pressure and coronary flow to decrease. These effects are magnified when contractility is increased by paired pacing.

It has been demonstrated that acceleration and deceleration of coronary flow is governed by the net wave intensity. During isovolumic contraction, the net backward-travelling compression wave (because there is no forward wave during this interval, the net intensity is equal to the intensity of the backward-travelling wave) is responsible for decrease coronary flow; the net forward-travelling compression wave (i.e., the sum of the intensities of the forward- and backward-travelling waves) is responsible for increasing coronary flow (after flow reaches its minimum) during

later systole, due to the increase in aortic pressure caused by LV ejection. Coronary blood flow is determined by the interaction of upstream aortic and downstream coronary microcirculatory events. During LV relaxation, decreasing elastance appears to generate forward-travelling expansion wave (via the aorta) and backward-travelling expansion wave (via the coronary vasculature). By separating upstream and downstream effects in this way, wave intensity analysis has demonstrated its advantages in enhancing our understanding of coronary flow dynamics.

As detailed in Chapter 5, the effects of changing coronary tone and LV contractility were investigated. It is shown that when contractility is relatively constant, decreasing coronary tone (by vasodilators) increases both the intensity of the backward-travelling compression wave and the coronary systolic flow impediment. When coronary tone is relatively constant, increasing contractility by paired pacing increases both the intensity of the backward-travelling compression wave and the coronary systolic flow impediment. The changes in coronary systolic flow impediment are inversely related to the changes of coronary vascular tone. We conclude that increasing LV contractility significantly increases the coronary systolic flow impediment and that the dilated coronary system increases the sensitivity of the response to myocardial contraction. The same extravascular force seems to cause a larger coronary flow reduction. The dilated coronary microcirculation might be better coupled to the myocardium and, thus, more susceptible to compression.

Coronary tone and LV contractility play an important role in modulating coronary blood flow. A better understanding of how the coronary microcirculation and LV contractility interact to determine coronary flow dynamics may be helpful for

patient management. Augmenting coronary systolic blood flow and a better balancing of the relation between LV contractility and coronary tone in order to optimize coronary blood flow could be critical to some patients, because vasodilatation seems to make coronary blood flow more vulnerable to systolic contraction. Future studies are required. Wave intensity analysis has shown itself to be a useful tool in the study coronary flow dynamics.

CHAPTER 7

FUTURE STUDIES

To further exploit the demonstrated advantages of wave intensity analysis, future studies in the following areas may be indicated.

7.1 Wave Intensity Analysis of Coronary Venous Flow

The coronary venous system drains the blood from myocardial capillaries to the right heart. Compared to the coronary arterial system, the coronary venous tree has received much less attention and from the functional viewpoint, the role of the venous bed may be subtle. However, studies have shown that coronary sinus occlusion and coronary venous retroperfusion benefit ischemic myocardium [18,33,34].

Wave intensity analysis may also be a useful tool to study coronary venous flow. Coronary venous flow increases during systole, while coronary inflow decreases [16]. In addition, coronary venous flow persists even after coronary arterial inflow cessation. To investigate the mechanism of this phenomenon, we can apply wave intensity analysis to the coronary vein. Coronary venous pressure and velocity can be measured by 2.5-F catheter-tip manometer (Millar) and Doppler Flowire respectively. We may predict that myocardial contraction will generate a forward-travelling compression wave (same direction as venous flow) in coronary venous vessels. This forward-travelling compression wave will propagate from small veins toward larger veins and it will increase coronary venous pressure and velocity. The amplitude of the forward-travelling compression wave may directly relate to LV contractility and coronary venous tone. Increasing LV contractility by paired pacing will increase the amplitude of forward-travelling compression wave, thus increasing

coronary venous flow. Because of better microcirculatory coupling, vasodilators may increases coronary venous flow by a larger forward-travelling compression wave.

Using wave intensity analysis, the mechanism by which obstruction of the coronary sinus increases coronary myocardial perfusion can be investigated as the function of backward-travelling wave.

7.2 Evaluation of Hemodynamic Changes after Intracoronary Stent Insertion

Intracoronary stents are being increasingly used for the treatment of patients with coronary artery disease. Intracoronary stent implantation significantly increases minimal luminal cross-sectional area, obstruction diameter, and decreases stenotic percentage. It prevents impending closure of the coronary lumen [77,110]. However, restenosis occurs in 20% to 30% of patient after successful intracoronary stent placement. In addition, there is a significant risk of thrombotic complications. [12,51,57]. It is not clear whether the risk of thrombosis and restenosis is due to the stimulation of the metallic foreign body or hemodynamic factors. Wave intensity analysis may be useful to investigate the hemodynamic changes after stent insertion and may be helpful to define the risk factors.

It has suggested that a larger acute increase in minimum lumen diameter may diminish the restenosis rate [57]. Some of the complications of subacute thrombosis or restenosis may be due to inadequate stent expansion during initial deployment [67]. Therefore, the determination of appropriate stent expansion is important.

Angiographic appearance and intravascular ultrasound imaging have been used as assessment of successful, angiographic imaging may not reveal the three-dimensional geometry that is necessary to appreciate the full expansion of a cylindrical meshwork device as intracoronary stent. Intravascular ultrasound provides detailed cross-sectional images within the vessel lumen, but do not provide potentially important information regarding hemodynamics. Wave intensity analysis, which is sensitive to diameter change and provides both upstream and downstream dynamic information and their interaction, may be an additional helpful tool in estimating successful stent implantation in coronary arteries.

7.3 Assessing Coronary Stenosis Severity and Coronary Vascular Properties

Assessing coronary stenosis severity is important in clinical management of patients with ischemic heart disease because the percentage of coronary diameter stenosis is directly related to physiologic significance [111]. The coronary angiogram has been used to assess coronary stenosis severity. Normal caliber coronary vessels with minimal irregularities are not significantly obstructed and nearly totally occluded vessels are significantly obstructed and, so, these therapeutic decisions are relatively easy. However, assessing the physiologic significance of narrowing of intermediate severity is much more tenuous.

Although percent diameter stenosis is very helpful in predicting the physiologic effects of an experimentally produced obstruction in an otherwise normal coronary vessel, the applicability of this index to clinical coronary disease, which usually is diffuse, has been seriously challenged. In addition, the percent stenosis alone or any

single stenosis dimension would not completely describe the physiological significance of an obstruction over a broad range of conditions, particularly, in lesions of intermediate severity.

Wave intensity analysis represents both pressure and velocity changes and reflects vascular properties. It assesses upstream and downstream effects as a whole subject, not only one specific segment. It may be sensitive in detecting diffuse coronary atherosclerosis, estimating intermediate severity stenosis and avoiding incorrectly assessed multivessel coronary disease.

Because coronary circulation is a complicated system and difficult to assess, wave intensity analysis may become a powerful tool in the study of coronary flow dynamics in both experimental and clinical investigations.

REFERENCES

1. Allaart CP, Westerhof N. Effect of length and contraction on coronary perfusion in isolated perfused papillary muscle of rat heart. Am J Physiol Heart Circ Physiol 1996; 271:H447-H454.

2. Armour JA, Klassen GA. Epicardial coronary venous pressure. Canad J Physiol Pharmacol 1981; 59:1250-1259.

3. Arts T, Kruger RTI, van Greven W, Lambregts JAC, Reneman RS. Propagation velocity and reflection of pressure waves in the canine coronary artery. Am J Physiol Heart Circ Physiol 1979; 237:H469-H474.

4. Arts T, Reneman RS. Interaction between intramyocardial pressure (IMP) and myocardial circulation. J Biomech Eng 1985; 107(1):51-56.

5. Ashikawa K, Kanatsuka H, Suzuki T, Takishima T. Phasic blood flow velocity pattern in epimyocardial microvessels in the beating canine left ventricle. Circ Res 1986; 59:704-711.

6. Bai XJ, Iwamoto T, Williams AG, Jr., Fan WL, Downey HF. Coronary pressure-flow autoregulation protects myocardium from pressure- induced changes in oxygen consumption. Am J Physiol 1994; 266(6 Pt 2):H2359-H2368.

7. Berne RM, Levy MN. Cardiovascular Physiology. 5th ed. St. Louis: The C. V. Mosby Company, 1986.

8. Bouma P, Sipkema P, Westerhof N. Coronary arterial inflow impediment during systole is little affected by capacitive effects. Am J Physiol Heart Circ Physiol 1993; 264:H715-H721.

9. Bouma P, Sipkema P, Westerhof N. Vasomotor tone affects diastolic coronary flow and flow impediment by cardiac contraction similarly. Am J Physiol Heart Circ Physiol 1994; 266:H1944-H1950.

10. Burkhoff D, Oikawa RY, Sagawa K. Influence of pacing site on canine left ventricular contraction. Am J Physiol Heart Circ Physiol 1986; 251:H428-H435.

11. Carew TE, Covell JW. Effect of intramyocardial pressure on the phasic flow in the interventricular septal artery. Cardiovasc Res 1976; 10:56-64.

12. Carrozza JP, Jr., Kuntz RE, Levine MJ, Pomerantz RM, Fishman RF, Mansour M, Gibson CM, Senerchia CC, Diver DJ, Safian RD, . Angiographic and clinical outcome of intracoronary stenting: immediate and long-term results from a large single-center experience. J Am Coll Cardiol 1992; 20(2):328-337.

13. Chilian WM. Functional distribution of alpha-1 and alpha-2 adrenergic receptors in the coronary microcirculation. Circ 1991; 84(5):2108-2122.

14. Chilian WM, Eastham CL, Marcus ML. Microvascular distribution of coronary vascular resistance in beating left ventricle. Am J Physiol 1986; 251(4 Pt 2):H779-88.

15. Chilian WM, Marcus ML. Phasic coronary blood flow velocity in intramural and epicardial coronary arteries. Circ Res 1982; 50:775-781.

16. Chilian WM, Marcus ML. Coronary venous outflow persists after cessation of coronary arterial inflow. Am J Physiol 1984; 247(6 Pt 2):H984-H990.

17. Chilian WM, Marcus ML. Effects of coronary and extravascular pressure on intramyocardial and epicardial blood velocity. Am J Physiol 1985; 248(2 Pt 2):H170-8.

18. Ciuffo AA, Guerci AD, Bukley G, Casale A, Weisfeldt ML. Intermittent obstruction of the coronary sinus following coronary ligation in dogs reduces ischemic necrosis and increases myocardial perfusion. In: Mohl W, Wolner E, Glogar D, editors. The Coronary Sinus. New York: Springer-Verlag, 1984: 454-464.

19. Danielle HB. Coronary flow alterations on myocardial contractility, oxygen extraction, and oxygen consumption. Am J Physiol 1973; 225:1020-1025.

20. Dankelman J, Stassen HG, Spaan JA. Interaction between Gregg's phenomenon and coronary flow control: a model study. Med Biol Eng Comput 1999; 37(6):742-749.

21. Dankelman J, Van der Ploeg CP, Spaan JA. Transients in myocardial O2 consumption after abrupt changes in perfusion pressure in goats. Am J Physiol 1996; 270(2 Pt 2):H492-H499.

22. DeFily DV, Patterson JL, Chilian WM. Endogenous adenosine modulates α_2- but not α_1-adrenergic constriction of coronary arterioles. Am J Physiol Heart Circ Physiol 1995; 268:H2487-H2494.

23. Di Mario C, Strikwerda S, Gil R, de Feyter PJ, de Jaegere P, Serruys PW. Response of conductance and resistance coronary vessels to scalar concentrations of acetylcholine: assessment with quantitative angiography and intracoronary Doppler echography in 29 patients with coronary artery disease. Am Heart J 1994; 127(3):514-531.

24. Domenech RJ. Regional diastolic coronary blood flow during diastolic ventricular hypertension. Cardiovasc Res 1978; 12(11):639-645.

25. Downey JM, Downey HF, Kirk ES. Effect of myocardial strains on coronary blood flow. Circ Res 1974; 34:286-292.

26. Downey JM, Kirk ES. Distribution of the coronary blood flow across the canine heart wall during systole. Circ Res 1974; 34:251-257.

27. Downey JM, Kirk ES. Inhibition of coronary blood flow by a vascular waterfall mechanism. Circ Res 1975; 36:753-763.

28. Flynn AE, Coggins DL, Goto M, Aldea GS, Austin RE, Doucette JW, Husseini W, Hoffman JIE. Does systolic subepicardial perfusion come from retrograde subendocardial flow? Am J Physiol Heart Circ Physiol 1992; 262(6):H1759-H1769.

29. Gow B, Schonfeld D, Patel DJ. The dynamic elastic properties of the canine left circumflex coronary artery. J Biomech 1974; 7:389-395.

30. Gregg DE. Effect of coronary perfusion pressure on coronary flow and oxygen usage of the myocardium. Circ Res 2001; 8:497-500.

31. Gregg DE, Green HD. Registration and interpretation of normal phasic inflow into a left coronary artery by an improved differential manometric method. Am J Physiol 1940; 130:114-125.

32. Griffith TM, Edwards DH. EDRF in intact vascular networks. Blood Vessels 1990; 27:230-237.

33. Gross L, Blum L, Silverman G. Experimental attempts to increase the blood supply to the dog's heart by means of coronary sinus occlusion. J Exp Med 1935; 65:91-106.

34. Gundry SR. Modification of myocardial ischemia in normal and hypertrophied hearts utilizing diastolic retroperfusion of the coronary veins. J Thorac Cardiovasc Surg 1982; 83(5):659-669.

35. Han Y, Vergroesen I, Goto M, Dankelman J, Van der Ploeg CP, Spaan JA. Left ventricular pressure transmission to myocardial lymph vessels is different during systole and diastole. Pflugers Arch 1993; 423(5-6):448-454.

36. Han Y, Vergroesen I, Spaan JAE. Stopped-flow epicardial lymph pressure is affected by left ventricular pressure in anesthetized goats. Am J Physiol Heart Circ Physiol 1993; 264:H1624-H1628.

37. Heineman FW, Grayson J. Transmural distribution of intramyocardial pressure measured by micropipette technique. Am J Physiol Heart Circ Physiol 1985; 249:H1216-H1223.

38. Hoffman JIE, Buckberg GD. Transmural variations in myocardial perfusion. Prog Cardiol 1976; 5:37-89.

39. Hollander EH. Wave-intensity analysis of pulmonary arterial blood flow in anesthetized dogs. University of Calgary, 1998.

40. Jones CJ, DeFily DV, Patterson JL, Chilian WM. Endothelium-dependent relaxation competes with alpha-1 and alpha-2 adrenergic constriction in the canine epicardial coronary microcirculation. Circ 1993; 87(4):1264-1274.

41. Jones CJ, Kuo L, Davis MJ, Chilian WM. Distribution and control of coronary microvascular resistance. Adv Exp Med Biol 1993; 346:181-8:181-188.

42. Jones CJH, Parker KH, Hughes R, Sheridan DJ. Nonlinearity of human arterial pulse wave transmission. J Biomech Eng 1992; 114:10-14.

43. Jones CJH, Sugawara M. "Wavefronts" in the aorta -- implications for the mechanisms of left ventricular ejection and aortic valve closure. Cardiovasc Res 1993; 27:1902-1905.

44. Jones CJH, Sugawara M, Davies RH, Kondoh Y, Uchida K, Parker KH. Arterial wave intensity: physical meaning and physiological significance. In: Hosoda S, Yaginuma T, Sugawara M, Taylor MG, Caro CG, editors. Recent Progress in Cardiovascular Mechanics. Chur, Switzerland: Harwood, 1994: 129-148.

45. Judd RM, Levy BI. Effects of barium-induced cardiac contraction on large- and small-vessel intramyocardial blood volume. Circ Res 1991; 68(1):217-225.

46. Kajiya F, Goto M, Yada T, Ogasawara Y, Tsujioka K. Mechanics of intramural blood vessels of the beating heart. In: Jaffrin MY, Caro CG, editors. Biological Flows. New York: Plenum Press, 1995: 255-265.

47. Kajiya F, Tomonaga G, Tsujioka K, Ogasawara Y, Nishihara H. Evaluation of local blood flow velocity in proximal and distal coronary arteries by laser Doppler method. J Biomech Eng 1985; 107(1):10-15.

48. Kajiya F, Tomonaga G, Tsujioka K, Ogasawara Y, Nishihara H. An optical-fiber laser blood flow velocity in proximal and distal coronary arteries by laser Doppler method. Trans ASME 1987; 107:10-15.

49. Kajiya F, Yada T, Kimura A, Hiramatsu O, Goto M, Ogasawara Y, Tsujioka K. Endocardial coronary microcirculation of the beating heart. Adv Exp Med Biol 1993; 346:173-180.

50. Kal JE, Van Wezel HB, Porsius M, Vergroesen I, Spaan JA. Metabolic coronary-flow regulation and exogenous nitric oxide in human coronary artery disease: assessment by intravenous administration of nitroglycerin. J Cardiovasc Pharmacol 2000; 35(1):7-15.

51. Kimura T, Nosaka H, Yokoi H, Iwabuchi M, Nobuyoshi M. Serial angiographic follow-up after Palmaz-Schatz stent implantation: comparison with conventional balloon angioplasty. J Am Coll Cardiol 1993; 21(7):1557-1563.

52. Klassen GA, Zborowska-Sluis DT. The effect of myocardial force on coronary transmural flow distribution. Cardiovasc Res 1979; 13:365-369.

53. Krams R, Sipkema P, Westerhof N. Varying elastance concept may explain coronary systolic flow impediment. Am J Physiol Heart Circ Physiol 1989; 257:H1471-H1479.

54. Krams R, Sipkema P, Westerhof N. Coronary oscillatory flow amplitude is more affected by perfusion pressure than ventricular pressure. Am J Physiol Heart Circ Physiol 1990; 258:H1889-H1898.

55. Krams R, Sipkema P, Zegers J, Westerhof N. Contractility is the main determinant of coronary systolic flow impediment. Am J Physiol Heart Circ Physiol 1989; 258:H1936-H1944.

56. Krams R, van Haelst ACTA, Sipkema P, Westerhof N. Can coronary systolic-diastolic flow differences be predicted by left ventricular pressure or time-varying intramyocardial elastance? Basic Res Cardiol 1989; 84:149-159.

57. Kuntz RE, Gibson CM, Nobuyoshi M, Baim DS. Generalized model of restenosis after conventional balloon angioplasty, stenting and directional atherectomy. J Am Coll Cardiol 1993; 21(1):15-25.

58. Kuo L, Davis MJ, Chilian WM. Longitudinal gradients for endothelium-dependent and -independent vascular responses in the coronary microcirculation. Circ 1995; 92:518-525.

59. Laughlin MH. Endothelium-mediated control of coronary vascular tone after chronic exercise training. Med Sci Sports Exerc 1995; 8:1135-1144.

60. Lee J, Chambers DE, Akizuki S, Downey JM. The role of vascular capacitance in the coronary arteries. Circ Res 1984; 55(6):751-762.

61. Lighthill MJ. Waves in Fluids. Cambridge: Cambridge University Press, 1978.

62. Marcus M, Wright C, Doty D, Eastham C, Laughlin D, Krumm P, Fastenow C, Brody M. Measurements of coronary velocity and reactive hyperemia in the coronary circulation of humans. Circ Res 1981; 49(4):877-891.

63. Marzilli M, Goldstein S, Sabbah HN, Lee T, Stein PD. Modulating effect of regional myocardial performance on local myocardial perfusion in the dog. Circ Res 1979; 45:634-641.

64. Mihailescu LS, Abel FL. Intramyocardial pressure gradients in working and nonworking isolated cat hearts. Am J Physiol Heart Circ Physiol 1994; 266:H1233-H1241.

65. Morita K, Mori H, Tsujioka K, Kimura A, Ogasawara Y, Goto M, Hiramatsu O, Kajiya F, Feigl EO. α-adrenergic vasoconstriction reduces systolic retrograde coronary blood flow. Am J Physiol Heart Circ Physiol 1997; 273:H2746-H2755.

66. Murphree SS, Saffitz JE. Delineation of the distribution of beta-adrenergic receptor subtypes in canine myocardium. Circ Res 1988; 63(1):117-125.

67. Nakamura S, Colombo A, Gaglione A, Almagor Y, Goldberg SL, Maiello L, Finci L, Tobis JM. Intracoronary ultrasound observations during stent implantation. Circ 1994; 89(5):2026-2034.

68. Nichols WW, O'Rourke MF. McDonald's Blood Flow in Arteries. 3rd ed. Philadelphia: Lea & Febiger, 1990.

69. Nishikawa Y, Stepp DW, Chilian WM. In vivo location and mechanism of EDHF-mediated vasodilation in canine coronary microcirculation. Am J Physiol Heart Circ Physiol 1999; 277(3):H1252-H1259.

70. Nishikawa Y, Stepp DW, Chilian WM. Nitric oxide exerts feedback inhibition on EDHF-induced coronary arteriolar dilation in vivo. Am J Physiol Heart Circ Physiol 2000; 279(2):H459-H465.

71. Pagliaro P, Paolocci N, Isoda T, Saavedra WF, Sunagawa G, Kass DA. Reversal of glibenclamide-induced coronary vasoconstriction by enhanced perfusion pulsatility: possible role for nitric oxide. Cardiovasc Res 2000; 45(4):1001-1009.

72. Pagliaro P, Senzaki H, Paolocci N, Isoda T, Sunagawa G, Recchia FA, Kass DA. Specificity of synergistic coronary flow enhancement by adenosine and pulsatile perfusion in the dog. J Physiol Lond 1999; 520(1):271-280.

73. Panerai RB, Chamberlain JH, Sayers BM. Characterization of the extravascular component of coronary resistance by instantaneous pressure-flow relationships in the dog. Circ Res 1979; 45(3):378-390.

74. Parker KH, Jones CJH. Forward and backward running waves in the arteries: analysis using the method of characteristics. J Biomech Eng 1990; 112:322-326.

75. Parker KH, Jones CJH, Dawson JR, Gibson DG. What stops the flow of blood from the heart? Heart and Vessels 1988; 4:241-245.

76. Petropoulakis PN, Kyriakidis MK, Tentolouris CA, Kourouclis CV, Toutouzas PK. Changes in phasic coronary blood flow velocity profile in relation to changes in hemodynamic parameters during stress in patients with aortic valve stenosis. Circ 1995; 92:1437-1447.

77. Puel J, Juilliere Y, Bertrand ME, Rickards AF, Sigwart U, Serruys PW. Early and late assessment of stenosis geometry after coronary arterial stenting. Am J Cardiol 1988; 61(8):546-553.

78. Rabbany SY, Kresh JY, Noordergraaf A. Assessment of intramyocardial fluid pressure with a fiber-optic sensor. FASEB J 1988; 2:A929-A929.

79. Rabbany SY, Kresh JY, Noordergraaf A. Intramyocardial pressure: interaction of myocardial fluid pressure and fiber stress. Am J Physiol Heart Circ Physiol 1989; 257:H357-H364.

80. Recchia FA, Senzaki H, Saeki A, Byrne BJ, Kass DA. Pulse pressure-related changes in coronary flow in vivo are modulated by nitric oxide and adenosine. Circ Res 1996; 79(4):849-856.

81. Resar J, Livingston JZ, Halperin HR, Sipkema P, Krams R, Yin FC. Effect of wall stretch on coronary hemodynamics in isolated canine interventricular septum. Am J Physiol 1990; 259(6 Pt 2):H1869-H1880.

82. Richmond KN, Tune JD, Gorman MW, Feigl EO. Role of K+ATP channels in local metabolic coronary vasodilation. Am J Physiol 1999; 277(6 Pt 2):H2115-H2123.

83. Richmond KN, Tune JD, Gorman MW, Feigl EO. Role of K(ATP)(+) channels and adenosine in the control of coronary blood flow during exercise. J Appl Physiol 2000; 89(2):529-536.

84. Ross J, Jr., Sonnenblick EH, Kaiser GA, Frommer PL, Braunwald E. Electroaugmentation of ventricular performance and oxygen consumption by repetitive application of paired electrical stimuli. Circ Res 1965; 16:332-342.

85. Rouleau J, Boerboom LE, Surjadhana A, Hoffman JI. The role of autoregulation and tissue diastolic pressures in the transmural distribution of left ventricular blood flow in anesthetized dogs. Circ Res 1979; 45(6):804-815.

86. Rumberger JA, Nerem RM, Muir WW, III. Coronary artery pressure development and wave transmission characteristics in the horse. Cardiovasc Res 1979; 13:413-419.

87. Sabiston DC, Jr., Gregg DE. Effect of cardiac contraction on coronary blood flow. Circ 1957; 15:14-20.

88. Sagawa K, Suga H, Shoukas AA, Bakalar KM. End-systolic pressure-volume ratio: a new index of ventricular contractility. Am J Cardiol 1977; 40:748-753.

89. Scott-Douglas NW, Traboulsi M, Smith ER, Tyberg JV. Experimental instrumentation and left ventricular pressure- strain relationship. Am J Physiol Heart Circ Physiol 1991; 261:H1693-H1697.

90. Shipley RE, Gregg DE. The effect of external constriction of a blood vessel on blood flow. Am J Physiol 1944; 141:289-296.

91. Sipkema P, Yamada H, Yin FC. Coronary artery resistance changes depend on how surrounding myocardial tissue is stretched. Am J Physiol 1996; 270(3 Pt 2):H924-34.

92. Snyder R, Downey JM, Kirk ES. The active and passive components of extravascular coronary resistance. Cardiovasc Res 1975; 9:161-166.

93. Spaan JAE. Coronary Blood Flow. Dordrecht: Kluwer Academic Publishers, 1991.

94. Spaan JAE. Nonlinear models of coronary flow mechanics. In: Jaffrin MY, Caro CG, editors. Biological Flows. New York: Plenum Press, 1995: 267-286.

95. Spaan JAE, Breuls PW, Laird JD. Diastolic-systolic coronary flow differences are caused by intramyocardial pump action in the anaesthetized dog. Circ Res 1981; 49:584-593.

96. Stein PD, Marzilli M, Sabbah HN, Lee T. Systolic and diastolic pressure gradients within the left ventricular wall. Am J Physiol Heart Circ Physiol 1980; 238:H625-H630.

97. Stein PD, Sabbah HN, Marzilli M, Blick EF. Comparison of the distribution of intramyocardial pressure across the canine left ventricular wall in the beating heart during diastole and in the arrested heart. Evidence of epicardial muscle tone during diastole. Circ Res 1980; 47:258-267.

98. Stepp DW, Nishikawa Y, Chilian WM. Regulation of shear stress in the canine coronary microcirculation. Circ 1999; 100(14):1555-1561.

99. Stewart JM, Wang J, Hintze TH. Role of EDRF in the regulation of shear rate in large coronary arteries in conscious dogs. J Mol Cell Cardiol 1994; 26:1625-1633.

100. Sudhir K, MacGregor JS, Barbant SD, Foster E, Fitzgerald PJ, Chatterjee K, Yock PG. Assessment of coronary conductance and resistance vessel reactivity in response to nitroglycerin, ergonomine and adenosine: in vivo studies with

simultaneous intravascular two-dimensional and Doppler ultrasound. J Am Coll Cardiol 1993; 21:1261-1268.

101. Suga H, Sagawa K. Instantaneous pressure-volume relationships and their ratio in the excised, supported canine left ventricle. Circ Res 1974; 35:117-126.

102. Suga H, Sagawa K, Shoukas AA. Load independence of the instantaneous pressure-volume ratio of the canine left ventricle and effects of epinephrine and heart rate on the ratio. Circ Res 1973; 32(3):314-322.

103. Sun Y-H, Anderson TJ, Parker KH, Tyberg JV. Wave-intensity analysis: a new approach to coronary dynamics. J Appl Physiol 2000; 89:1636-1644.

104. Sun Y-H, Anderson TJ, Tyberg JV. Effects of coronary vascular tone and myocardial compression on systolic coronary flow reduction. Journal of Cardiovascular Diagnosis and Procedures 13, 288. 1996.
Abstract

105. Trimble J, Downey J. Contribution of myocardial contractility to myocardial perfusion. Am J Physiol Heart Circ Physiol 1979; 236:H121-H126.

106. Tune JD, Richmond KN, Gorman MW, Feigl EO. Role of Nitric Oxide and Adenosine in Control of Coronary Blood Flow in Exercising Dogs. Circ 2000; 101(25):2942-2948.

107. Tyberg JV, MacRae JM, Isaac DL, Dobson GM, Sun Y-H. Left ventricular filling dynamics: application of wave-intensity analysis. Journal of

Cardiovascular Diagnosis and Procedures 12, 122. 1994.

Abstract

108. van Huis GA, Sipkema P, Westerhof N. Coronary input impedance during cardiac cycle as determined by impulse response method. Am J Physiol Heart Circ Physiol 1987; 253:H317-H324.

109. Vatner DE, Knight DR, Homcy CJ, Vatner SF, Young MA. Subtypes of beta-adrenergic receptors in bovine coronary arteries. Circ Res 1986; 59(4):463-473.

110. Versaci F, Tomai F, Nudi F, Gaspardone A, De Fazio A, Ciavolella M, Crea F, Mango L, Chiariello L, Gioffre PA. Differences of regional coronary flow reserve assessed by adenosine thallium-201 scintigraphy early and six months after successful percutaneous transluminal coronary angioplasty or stent implantation. Am J Cardiol 1996; 78(10):1097-1102.

111. White CW, Creighton BW, Doty DB, Hiratza LF, Eastham CL, Harrison DG, Marcus ML. Does visual interpretation of the coronary arteriogram predict the physiologic importance of a coronary stenosis? N Engl J Med 1984; 310:819-824.

112. Wiggers CJ. Cardiac mechanisms that limit operation of ventricular suction. Science 1957; 126:1237.

113. Wusten B, Buss DD, Deist H, Schaper W. Dilatory capacity of the coronary circulation and its correlation to the arterial vasculature in the canine left ventricle. Basic Res Cardiol 1977; 72(6):636-650.

114. Yada T, Richmond KN, van Bibber R, Kroll K, Feigl EO. Role of adenosine in local metabolic coronary vasodilation. Am J Physiol 1999; 276(5 Pt 2):H1425-H1433.

115. Zhao G, Zhang XP, Xu XB, Ochoa M, Hintze TH. Short-term exercise training enhances reflex cholinergic nitric oxide-dependent coronary vasodilation in conscious dogs. Circ Res 1997; 80(6):868-876.